



The continental lithosphere: Reconciling thermal, seismic, and petrologic data

Irina M. Artemieva*

Geological Institute, University of Copenhagen, Denmark

ARTICLE INFO

Article history:

Received 8 May 2008

Accepted 20 September 2008

Available online 1 November 2008

Keywords:

Lithospheric mantle

Cratons

Heterogeneity

Kimberlites

Metasomatism

Lithosphere thickness

Lithosphere–asthenosphere boundary

ABSTRACT

The goal of the present study is to extract non-thermal signal from seismic tomography models in order to distinguish compositional variations in the continental lithosphere and to examine if geochemical and petrologic constraints on global-scale compositional variations in the mantle are consistent with modern geophysical data. In the lithospheric mantle of the continents, seismic velocity variations of a non-thermal origin (calculated from global V_s seismic tomography data [Grand S.P., 2002. Mantle shear-wave tomography and the fate of subducted slabs. *Philosophical Transactions of the Royal Society of London. Series A*, 360, 2475–2491.; Shapiro N.M., Ritzwoller M.H. 2002. Monte-Carlo inversion for a global shear velocity model of the crust and upper mantle. *Geophysical Journal International* 151, 1–18.] and lithospheric temperatures [Artemieva I.M., Mooney W.D., 2001. Thermal structure and evolution of Precambrian lithosphere: A global study. *Journal of Geophysical Research* 106, 16387–16414.] show strong correlation with tectono-thermal ages and with regional variations in lithospheric thickness constrained by surface heat flow data and seismic velocities. In agreement with xenolith data, strong positive velocity anomalies of non-thermal origin (attributed to mantle depletion) are clearly seen for all of the cratons; their amplitude, however, varies laterally and decreases with depth, reflecting either a peripheral growth of the cratons in Proterozoic or their peripheral reworking. These cratonic regions where kimberlite magmas erupted show only weakly positive compositional velocity anomalies, atypical for the “intact” cratonic mantle. A reduction in the amplitude of compositional velocity anomalies in kimberlite provinces is interpreted to result from metasomatic enrichment (prior or during kimberlite emplacement) of the cratonic mantle, implying that xenolith data maybe non-representative of the “intact” cratonic mantle.

© 2008 Elsevier B.V. All rights reserved.

1. Introduction

The concept of a solid, non-deformable outer layer of the Earth (initially estimated to be about 100 km thick) and its fluid, deformable interior has appeared as a result of the early gravity studies of the 18th–19th centuries, although the term “lithosphere” did not come into existence until the late 19th–early 20th century (see Watts (2001) for a detailed review). Soon afterwards, the term “asthenosphere” was introduced (Barrel, 1914) to describe a fluid, deformable layer (initially estimated as several hundred kilometers thick) below the “lithosphere”. With the booming development of seismological methods in the first half of the 20th century, which led to a discovery of the seismic low velocity zone (the LVZ) at 100–150 km depth (Gutenberg, 1954) and its base (the Lehmann discontinuity) at ca. 220 km depth (Lehmann, 1961, 1962), the term “lithosphere” acquired a new, seismic, justification. Since, surprisingly, the top of the seismic LVZ was found to be at about the same depth as the transition between solid outer layer of the Earth (the “lithosphere”) and its low-viscous, deformable interior (the “asthenosphere”), as defined from early

isostatic gravity models, it was tempting to explain both gravity and seismic observations by the same physical mechanisms.

The first heat flow measurements have been initiated more than a century ago by Everett (1883), with the first modern measurements of the terrestrial heat flow reported in the late 1930's for the continents and in the 50's for the oceans (Benfield, 1939; Bullard, 1939; Krige, 1939; Revelle and Maxwell, 1952). Maturation of geothermics as an independent technique to assess the physical state of the deep Earth's interior allowed the calculation of crustal and upper mantle geotherms for a large range of continental and oceanic regions (e.g. Jaeger, 1965; McKenzie, 1967). Combined with experimental and theoretical studies of the mantle composition and melting conditions in the upper mantle (Uffen, 1952; Ito and Kennedy, 1967; Kushiro et al., 1968), mantle geotherms were employed to explain the seismic LVZ in terms of peridotite partial melting. It was a big step forward as it allowed observations, which came from independent fields of geophysics, to be incorporated into a joint picture of the physical state of the upper mantle. Thus, the term “lithosphere” acquired an additional interpretation.

Further development of geophysical techniques and a gradual accumulation of extensive data sets in seismic, thermal, electromagnetic, rheological, and petrologic studies has led to much controversy in the use of the term “lithosphere”. Although the term became a

* Tel.: +45 4675 2438.

E-mail address: irina@geo.ku.dk.

convenient and widely used concept in geosciences, some authors argue that at present “it has become an unnecessarily confusing concept” (Anderson, 1995) due to an excessive number of different definitions of the “lithosphere”. Indeed, depending on the geophysical techniques (and physical properties measured), the lithosphere has different practical definitions. Most of them (i.e. seismic, electrical, elastic) are based on a sharp change in temperature-dependent physical properties at the transition from conductive (and rheologically strong) to convecting (and rheologically weak) upper mantle and thus crucially depend on the thermal regime of the upper mantle (Fig. 1).

This paper starts with a brief review of different concepts and definitions of the lithosphere. It then compares global thermal and seismic tomography models of the structure of the continental lithospheric mantle (CLM). Such a multi-data approach permits to specify the robust characteristics of the continental lithosphere and its evolution since the Archean. Data on the thermal regime of stable continental lithosphere provides exceptional information on lithospheric properties as it permits us to separate thermal and non-thermal effects in global geophysical models, such as seismic tomography. The goal of the present study is to perform a joint analysis of seismic and thermal data in order to extract a non-thermal signal from seismic models and to distinguish compositional (both vertical and lateral) variations in the CLM. This approach provides a basis for comparing the thickness of the continental lithosphere as

defined by seismic, thermal, and compositional variations. The conclusions of the study are then compared with the results of petrologic studies of mantle peridotites. Since xenoliths provide random, uneven, and in many areas sparse sampling of the Earth's deep interior, it is challenging to examine if geochemical constraints on global-scale compositional variations in the mantle are consistent with modern geophysical data.

2. What is the lithosphere?

2.1. Some semantics

In the classical, plate tectonics definition, the “lithosphere” is the upper rigid layer, which moves mechanically coherently with plate motions (the *mechanical boundary layer*, MBL). The base of the MBL is commonly interpreted as being associated with mantle zones of reduced viscosity and asthenospheric flow and, in petrologic studies, is constrained by variations in texture of xenoliths (sheared or non-sheared) brought to the surface from different depths in the mantle (Nixon and Boyd, 1973). Since mantle viscosity is strongly temperature-dependent, the thickness of the MBL should be proportional to the thickness of the *thermal boundary layer* (TBL, i.e. the layer with dominating conductive heat transfer above the convecting mantle), unless weak mantle rheology is caused by presence of fluids.

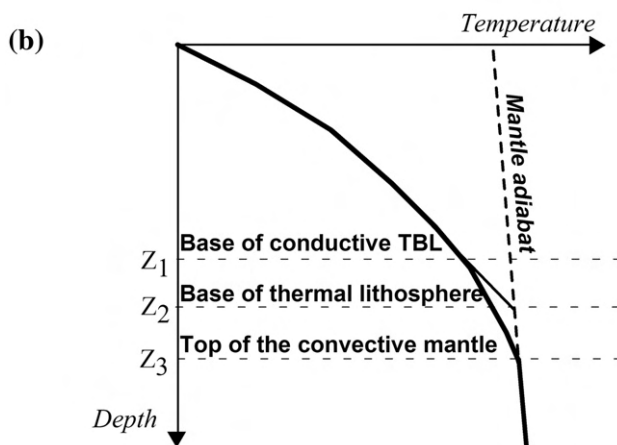
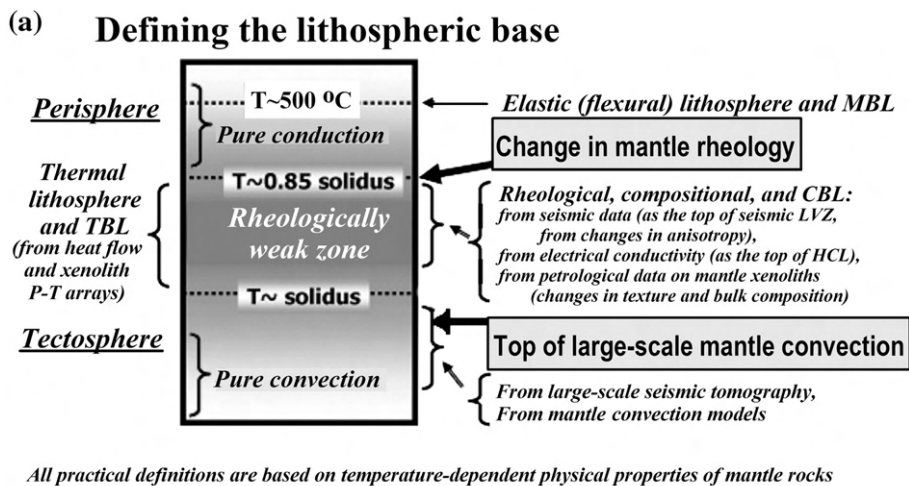


Fig. 1. (a) Different definitions of the lithospheric base, which are widely used in geophysics: thermal, seismic, rheological, electrical, elastic. All of these definitions are based on different temperature-dependent physical properties of the upper mantle rocks. However, there is a significant difference in lithospheric thickness as defined by different methods. See text for explanations. (b) Relationships between thicknesses of thermal boundary layer (z_1), thermal lithosphere (for simplicity calculated as the depth z_2 where a linear continuation of the geotherm intersects a mantle adiabat), and seismic lithosphere (z_3) (modified after Jaupart and Mareschal, 1999).

Depth variations of mantle composition sampled by mantle-derived xenoliths provide information on the thickness of the *chemical boundary layer* (CBL), or *petrologic lithosphere*. This concept is widely used in studies of cratonic regions, where the base of the petrologic lithosphere can, for example, be “determined by the change from depleted (lithospheric) to undepleted (asthenospheric) trace-element signatures in garnet” (Griffin and Ryan, 1995). Numerous petrologic studies of xenoliths from the Archean-Proterozoic cratons of Africa (Kaapvaal, Zimbabwe, and Tanzania cratons), Siberia, Europe (Baltic Shield), Canada (Superior and Slave cratons), and South America (Guyana craton) indicate that the depth of the transition from depleted to undepleted mantle composition often coincides with the depth to the isotherm of ca. 1200–1300 °C and thus is close to the depth where a continental conductive geotherm intersects the mantle adiabat. Thus, in some cratonic regions, the petrologic and thermal lithosphere (i.e. CBL and TBL) may have similar thicknesses. Note that in some petrologic definitions (e.g. based on Y-depleted garnet concentrations), the base of the lithosphere appears to be a significantly non-isothermal boundary with temperature variations at the lithospheric base (strictly speaking, the base of the CBL) ranging from 950 °C to 1250 °C over lateral distances of ca. 100–200 km (Griffin et al., 1999a). These huge short-wavelength temperature variations at the base of the CBL preclude a physically meaningful comparison of thus defined “lithospheric thickness” with lithospheric thickness estimated by geophysical methods (e.g. seismic, magnetotelluric, thermal), in which the base of the lithosphere (or the lithosphere–asthenosphere boundary, LAB) is defined by a sharp change of temperature-dependent physical properties of the upper mantle. Note that the base of the geophysically-defined lithosphere should not necessarily be isothermal, since anomalies in mantle composition and the presence of fluids affect physical properties of the lowermost lithospheric mantle measured in geophysical surveys; stress and basal drag in the lower lithosphere can further enhance its non-isothermal structure (e.g. Artemieva and Mooney, 2002; Garfunkel, 2007).

Two more concepts, the tectosphere and the perisphere, have been introduced as alternatives to the classical concepts of the lithosphere and asthenosphere. Although they are somewhat close in their meanings to the CBL, they differ significantly from the petrologic lithosphere as defined by compositional variations in cratonic xenoliths. The term “*perisphere*” (Anderson, 1995) is primarily geochemical concept, according to which the strong lithosphere extends down to the 600±50 °C isotherm and thus it is close to the MBL and is approximately twice thinner than the TBL (Fig. 1). In the early 1970's, a systematic difference between continents and oceans, persisting well below the LVZ, down to at least 400–500 km depth, was found from the analysis of surface-wave dispersion curves. It led Jordan (1975) to the “*tectosphere*” hypothesis, according to which the tectosphere is the layer, at least 400 km thick, (a) “which translates coherently in the course of horizontal plate motions”, (b) is dominated by a conductive heat transfer, and (c) is compositionally inhomogeneous so that “regions of lower potential temperature consist of material with intrinsically lower densities”. The latter assumption was further developed into the “*isopycnic*” (i.e. equal-density) hypothesis: the absence of geoid anomalies over the cratonic regions with thick lithospheric roots and cold geotherms led Jordan (1978) to suggest that the cratonic upper mantle has a low-density composition, the gravitational effect of which is compensated by low temperatures. Numerous petrologic studies of mantle xenoliths from different continental locations (e.g. Boyd and McCallister, 1976; Boyd, 1989; Griffin et al., 1998; Boyd et al., 1999; Lee and Rudnick, 1999) have confirmed the existence of systematic variations in the composition of the lithospheric mantle (due to depletion of the cratonic mantle in basaltic components, primarily Fe and Al), which result in a systematic increase in the upper mantle density (at standard *P–T* conditions, SPT) from ca. 3.31–3.33 t/m³ in the Archean cratons to 3.33–3.35 t/m³ in

Proterozoic mobile belts and to ca. 3.36 t/m³ in Phanerozoic regions (Jordan, 1988, 1997; Griffin et al., 1999b).

2.2. Defining the lithospheric base

While the top of the lithosphere, obviously, coincides with the topographic surface, it is not an easy task to define the lithospheric base as definitions depend on the geophysical technique. Four definitions of the lithosphere, *elastic, thermal, electrical, and seismic*, are widely used in geophysical studies. As it is clear from their names, they are based on indirect measurements of different properties of upper mantle rocks and thus they may refer to outer layers of the Earth with a significantly different thickness.

The concept of *elastic (flexural) lithosphere* (an elastic plate overlying viscous mantle) is close to the classical lithosphere definition, being related to the mechanical strength of the plate and referring to a rheologically strong layer which provides the isostatic response of the plate to topographic and/or subsurface loads (i.e. due to variations in crustal thickness and density) and mechanically supports elastic (far-field subhorizontal) stresses induced by lithospheric bending (flexure). The elastic thickness of the lithosphere, T_e , is the measure of mechanical strength of an elastic plate deflected by topographic and internal loads. This definition implies that the lithosphere has elastic rheology and thus, from a rheological point of view, the base of the elastic lithosphere corresponds to the elastic–plastic transition (Bodine et al., 1981). For mantle with the rheology of olivine, the critical isotherm for brittle–ductile transition is ~550 °C (Kusznir and Karner, 1985). Indeed, in continental regions the values of T_e generally depend on the tectono-thermal age (i.e. the time since the last major tectono-thermal event) (Artemieva, 2006) and range from 4 km in the Cenozoic Basin and Range Province (Bechtel et al., 1990) to ca. 100 km in the Precambrian platforms (Bechtel et al., 1990; Watts et al., 1995; Wang and Mareschal, 1999), with the base of the elastic (mechanical) lithosphere corresponding to the depth to 450–600 °C isotherm (Watts, 1978; De Rito et al., 1986). Thus the elastic lithosphere is approximately twice as thin as the thermal, seismic, and electrical lithospheres, the thicknesses of which are effectively controlled by lithospheric temperatures close to mantle adiabat (or solidus) (Table 1).

All practical definitions of the base of the lithosphere are based on temperature-dependent physical properties of mantle rocks indirectly measured in geophysical surveys (Fig. 1a). From this point of view, the definition of the *thermal lithosphere* (or TBL – the layer with dominating conductive heat transfer above the convecting mantle) is the most straightforward. The base of the TBL is commonly defined by the depth to a constant isotherm (e.g. 1300 °C) (McKenzie, 1967), or by the depth of the intersection of a continental geotherm either with a mantle adiabat (usually with the potential temperature in the range 1250–1350 °C since higher temperatures (1400–1450 °C) are inconsistent with laboratory data on *P–T* conditions at 410 km depth (Katsura et al., 2004)) or with a temperature close to mantle solidus (Pollack and Chapman, 1977). The choice of the latter is supported by laboratory studies of physical properties of mantle rocks at high *P–T* conditions (e.g. Sato and Sacks, 1989; Sato et al., 1989) which indicate a sharp change in rheology and elastic properties of olivine-rich rocks at temperatures between 0.85 T_m and T_m (where T_m is solidus temperature). Note, that the thickness of the TBL should not necessarily coincide with the thickness of the thermal lithosphere: a gradual transition from convection to conduction mechanisms of heat transfer in the mantle leads to an existence of a depth interval where mantle temperature becomes asymptotically close to mantle adiabat (its possible physical origins are discussed by Jaupart and Mareschal, 1999). In practice, a linear continuation of the geotherm in this depth interval to its intersection with a mantle adiabat is commonly used to estimate the lithospheric thermal thickness (Fig. 1b).

For stable continental regions, where thermal equilibrium has been established since the last major thermo-tectonic event,

Table 1
Typical properties of continental lithosphere of different ages

Age (for geophysical data)	Archean (>2.5 Ga)	Proterozoic (0.57–2.5 Ga)	Phanerozoic (<570 Ma)	Refs
Age (for xenolith-based data)	Archon (>2.5 Ga)	Proton (1.0–2.5 Ga)	Tecton (<1.0 Ga)	G99
Fo ₁₀₀ =Mg/[Mg+Fe]	92–94	91.5–92.5	90	G00
Mean mg#	92.7	90.6	89.9	G99, D01
Mean mode: ol/opx/cpx/gnt	69/25/2/4 (gnt CLM)	70/15/7/8 (gnt CLM)	60/17/11/12 (gnt CLM)	G99
		70/17/6/7 (xenoliths massifs)	66/17/9/8 (sp. peridotite)	
Mean V_p (SPT), km/s	8.34	8.32	8.30	G99
δV_p (%) compared to primitive mantle ($V_p=8.33$ km/s)	+0.1%	-0.1%	-0.4%	
Mean V_s (SPT), km/s	4.88	4.84	4.82	G99
δV_s (%) compared to primitive mantle ($V_s=4.81$ km/s)	+1.5%	+0.6%	+0.2%	
Mean density (SPT), g/cc	3.31±0.016	(3.33–3.35)±0.02	(3.36–3.37)±0.02	G99, D01
$\delta\rho$ (%) compared to primitive mantle ($\rho=3.39$ g/cc)	-2.4%	-1.2 to -1.8%	-0.6 to -0.9%	
Surface heat flow, mW/m ²	40–50 (group A)	40–60 (ePt)	50–70 (Pz)	P93
	20–45 (group B)	60–75 (lPt)	70–120 (Mz-Cz)	
Crustal thickness, km	32–40 (group A)	40–50	25–35 (extensional);	M05
	40–50 (group B)		35–70 (orogens)	
Moho temperature, °C	300–500	450–650 (ePt)	700–850 (Pz)	A06
		700–850 (lPt)	700–1000 (Mz-Cz)	
gradT in CLM, °C/km	4–5	5–7 (ePt)	7–11 (Pz),	A06
		8–11 (lPt)	10–25 (Mz-Cz)	
Thickness of thermal boundary layer, km	170–250 (group A)	140–220 (ePt)	80–140 (Pz);	AM01
	250–350 (group B)	90–120 (lPt)	60–100 (Mz-Cz, excluding slabs beneath Cz orogens)	
Thickness of chemical boundary layer, km	180–250	150–180	60–140	D01
Thickness of electrical lithosphere, km	150–270	150–250	70–130 (Pz);	A06
			<100 (Mz-Cz)	
Thickness of mechanical boundary layer, km	35–115	35–100 (ePt)	8–85 (Pz),	W99
		27–50 (mPt-lPt)	4–37 (Cz extensional), 35–90 (Cz orogens)	

Notes: (1) unless the opposite is indicated, the values in the Table show the typical ranges of the parameters, but not their averages; (2) by the lithospheric structure, Archean has been subdivided into two groups; group A=Western Australia, India, South Africa, South America (Sao Francisco and Rio de la Plata cratons); group B=Siberia, Baltic shield, Canadian Shield, West Africa (Artemieva and Mooney, 2001; Artemieva, 2006); (3) xenolith constraints on the CLM composition, modes, seismic velocities and density refer to slightly different age groups of >2.5 Ga, 1.0–2.5 Ga, and <1.0 Ga.

References: AM01=Artemieva and Mooney, 2001; A06=Artemieva, 2006; A04=Artemieva et al., 2006; G00=Gaul et al., 2000; G99=Griffin et al., 1999b; D01=Djomani et al., 2001; M05=derived from the global USGS crustal database (courtesy of W. Mooney, 2005); P93=derived from global heat flow database (Pollack et al., 1993); W99=based on compilation of Watts (1999), updated for missing and post-1999 publications.

Abbreviations: ePt=Paleoproterozoic, mPt=Mesoproterozoic, lPt=Neoproterozoic, Pz=Paleozoic, Mz-Cz=Meso-Cenozoic.

lithospheric geotherms are constrained by surface heat flow measurements and are calculated from a solution of the steady state conductivity equation. However, the approach is not valid for active regions, where lithospheric temperatures should be constrained by non-steady state thermo-dynamical models.

Mantle xenoliths are also used to constrain mantle temperatures. The approach proposed by Boyd (1973) is based on calculation of equilibrium P - T conditions for different mineral systems and provides another estimate of the *thermal lithospheric thickness* (Fig. 2). Due to a significant discrepancy between mantle pressures and temperatures constrained by different sets of geothermobarometers (sometimes reaching ± 10 kBar and 100 °C for the same rock samples, Grutter and Moore, 2003), the thickness of the thermal lithosphere is constrained non-uniquely by xenolith P - T arrays and its value should not necessarily agree with lithospheric thickness based on heat flow data.

Another approach to calculate upper mantle temperatures, and thus the thickness of the thermal lithosphere, is based on temperature-dependence of seismic velocities. Laboratory measurements of elastic parameters (e.g. Duffy and Anderson, 1989; Jackson et al., 1990) and theoretical (e.g. Karato, 1993) and experimental (Karato and Spetzler, 1990 and references therein) constraints on elastic and non-elastic behavior of mantle rocks at high P - T conditions provide the basis for velocity-temperature conversions. Although most of the recent models of this type take into account frequency-dependent anelastic effects (dissipation) (Karato, 1993; Faul and Jackson, 2005), the effects of partial melt (which strongly depend on melt geometry and water presence), fluids, seismic anisotropy, and compositional variations on seismic velocities are difficult to account for (e.g. Popp and Kern, 1993; Sobolev et al., 1996; Deschamps et al., 2002; McKenzie et al., 2005). Despite all of the difficulties, velocity-temperature inversions have been applied to high-resolution regional seismic tomography and seismic refraction models to estimate lithospheric temperatures in Europe (Furlong et al., 1995; Sobolev et al., 1996; Goes

et al., 2000), North America (Goes and van der Lee, 2002; Godey et al., 2004; Perry et al., 2006), Australia (Goes et al., 2005), and South Africa (Kuskov et al., 2006). Although these studies provide useful constraints on lithospheric thickness (derived from calculated geotherms), they should be treated with caution as they can lead to physically meaningless solutions with short-wavelength contrasts in mantle temperatures (e.g. Goes et al., 2000), in particular in the regions with contrasting properties of the lithosphere, where horizontal heat transfer has a smearing effect on lithospheric temperatures (Pinet and Jaupart, 1987), while seismic velocities can exhibit a sharp contrast. Furthermore, in the upper 200 km of the Earth, the correlation coefficient between seismic Rayleigh wave velocities and temperatures is less than 0.40 beneath the continents,

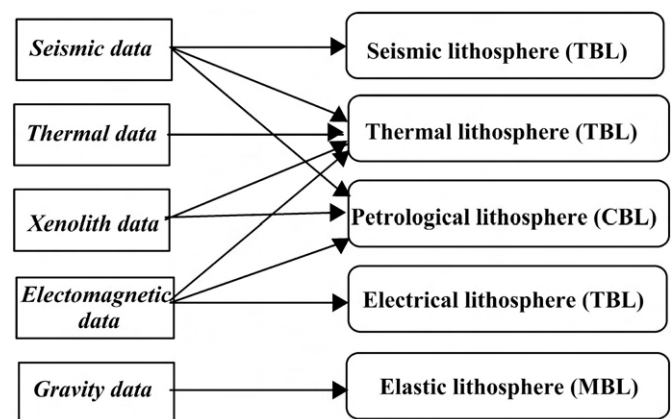


Fig. 2. Simplified scheme of the interlinks between methods of the upper mantle studies and the lithosphere definitions.

at least in part due to strong compositional and structural heterogeneity of the mantle, anelasticity, and presence of melts and fluids (Artemieva et al., 2004); these effects are difficult to incorporate into velocity–temperature conversions.

Changes in physical properties of mantle rocks measured in indirect geophysical surveys provide the basis for other definitions of the base of the lithosphere. They are supported by laboratory measurements of density, elastic moduli, and electrical conductivity of mantle rocks, parameters that have a strong temperature-dependence and a sharp change in properties at temperatures close to solidus (Murase and Fukuyama, 1980; Sato et al., 1989; Constable et al., 1992). According to the classical definition, *seismic lithosphere*, or the lid, is a seismic high-velocity layer above the low-velocity zone or above a zone of high velocity gradient in the upper mantle, presumably caused by partial melting. Note that when seismic models are constrained not in the absolute but in relative velocities (i.e. as a velocity perturbation with respect to a reference model), thus defined seismic LAB may be misleading (e.g. Priestley and Debayle, 2003), in particular when the PREM model (with a sharp velocity change at 220 km depth, typical for the oceanic lithosphere, but not required by seismic data for the continental regions) is used as a reference model for the continents (M. Cara, personal communication, 2002; Kennett, 2006).

The base of the *electrical lithosphere*, which is the highly resistive upper layer above highly conducting asthenosphere, is estimated from a sharp change in mantle conductivity (resistivity) associated perhaps with the presence of partial melt (although the presence of a high-conducting phase such as graphite may produce a similar effect). As with seismic velocity–temperature conversions, the strong temperature dependence of electrical conductivity of olivine can be used to estimate regional geotherms from magnetotelluric field observations (Ledo and Jones, 2005).

Asthenospheric flow and shear in the rheologically weak layer below the lithosphere produce alignment of minerals (including olivine which is highly anisotropic). It causes (a) changes in texture of mantle-derived peridotites at the transition from the lithosphere to the rheologically weak layer underneath it (associated with the base of the *petrologically constrained MBL*; the thickness of the transition zone is 20–25 km (Garfunkel, 2007)) and (b) seismic anisotropy, leading to one more definition of the base of *seismic lithosphere* as the depth where the axis of anisotropy changes its orientation (e.g. Plomerová et al., 2002).

Several other approaches (e.g. large-scale tomography models) treat the base of the lithosphere as the top of large-scale mantle convection (Sleep, 2003). As mentioned above, the existence of the transitional layer in the mantle, where the mode of heat transfer changes gradually from conduction to convection, leads to a significant difference in lithospheric thickness constrained “from the top” and “from the bottom” (Fig. 1a): lithospheric thickness estimated from large-scale seismic tomography models, which are sensitive to velocity anomalies associated with convective mantle, may extend some tens of kilometers deeper than the TBL (Jaupart and Mareschal, 1999).

This introduction clearly shows the reasons for Anderson (1995) to call the term *lithosphere* “an unnecessarily confusing concept”. Alternatively, one may argue that because of the complexity of the concept and because of its multi-disciplinary nature, the concept of the lithosphere is “necessarily confusing”. A great deal of confusion arises not only from the fact that different “lithospheres” (seismic, thermal, electrical, petrologic, flexural) are distinguished, but also from the fact that the same very terms are used in approaches utilizing different techniques (Fig. 2). Since these techniques often assess different physical properties of mantle rocks, they may refer to different phenomena and thus to different depth intervals in the upper mantle. “*Thermal lithosphere*” is a good example, since continental geotherms constrained by surface heat flow measurements, models of mantle convection, xenolith *P–T* arrays, velocity–

temperature and electrical conductivity–temperature conversions may disagree outside the uncertainty ranges for these methods (Figs. 1, 2). Thus, any discussion of lithospheric structure (including lithospheric thickness) is misleading without a clear statement that defines physical properties of the upper mantle that are considered, the techniques that are used to quantify them, and the definitions of the LAB that are employed. Here the term “lithosphere” is used to define the outer, rheologically strong layer of the Earth, that includes the crust and the uppermost (lithospheric) mantle and moves together with continental plates. The set of physical properties of the upper mantle, which defines the lithospheric base, is discussed for each interpretation technique used in the study.

3. Thermal versus seismic lithosphere

3.1. Thermal regime of the CLM

Data on surface heat flow, together with data on the crustal structure, thermal properties of crustal and mantle rocks, and geological and tectonic information, can be interpreted in terms of the thermal structure of the continental lithosphere (Artemieva and Mooney, 2001). For the cratonic regions that have not experienced a major tectonic event since the end of the Precambrian (Fig. 3) (Artemieva, 2006), the thermal structure of the lithosphere can be approximated by the steady-state solution of thermal conductivity equation. Indeed, the thermal front associated with a thermal anomaly at a depth z reaches the surface and becomes reflected in the surface heat in time $\tau = z^2/\chi$, where χ is thermal diffusivity. For $\chi = 10^{-6} \text{ m}^2/\text{s}$, this time is ca. 200 Ma and ca. 450 Ma for $z = 80 \text{ km}$ and 120 km , respectively. It means that steady-state approximation is also valid for platform regions affected by Paleozoic tectono-magmatic events where thermal equilibrium is expected to be re-established. [note that secular cooling of the Earth together with radioactive decay of heat-producing elements implies that any steady-state thermal formulation is an approximation for the real Earth (Michaut and Jaupart, 2007)].

The steady-state approximation allows us to calculate lithospheric geotherms from surface heat flow if the depth distribution of thermal properties (heat production and thermal conductivity) is known. The first calculations of the crustal and upper mantle geotherms were done for several continental and oceanic regions half a century ago (e.g. Jaeger, 1965; McKenzie, 1967). The next, significant step forward, was made by Pollack and Chapman (1977), who built their results on the idea of “heat flow provinces”. Based on empirical observations on a limited dataset, Birch et al. (1968) and Roy et al. (1968) recognized some useful relationships to constrain continental geotherms: a linear relationship between surface heat flow Q_0 and near-surface radioactivity A_0 ($Q_0 = Q_r + D A_0$), as is found in several continental regions, formed the basis for the concept of “heat flow provinces”. Later studies (e.g. several papers published in Geophysical Research Letters, v. 14, 1987) cast doubt on this relationship and demonstrated that it is not valid in regions with highly heterogeneous crustal structure. However, as shown by other papers in the same volume and by recent geothermal studies (Perry et al., 2006), it still remains useful when regions with the same tectonic evolution, similar geological structure, and with lateral dimensions $> 100 \text{ km}$ (i.e. greater than the wavelength of surface heat flow variations caused by crustal heterogeneity) are treated as “heat flow provinces”. The physical meaning of the constants Q_r (“reduced heat flow”) and D (“characteristic depth”) permits several interpretations. In one of them (Roy et al., 1968), D is interpreted as the thickness of a layer with a uniform radioactivity (approximately limited to the upper crust); however this interpretation fails in many tectonic regions and the value of D does not show correlation with crustal ages or any other crustal properties (Artemieva and Mooney, 2001). On the contrary, “ Q_r must have a general geophysical significance for old continental crust” (Sclater et al., 1980), where it

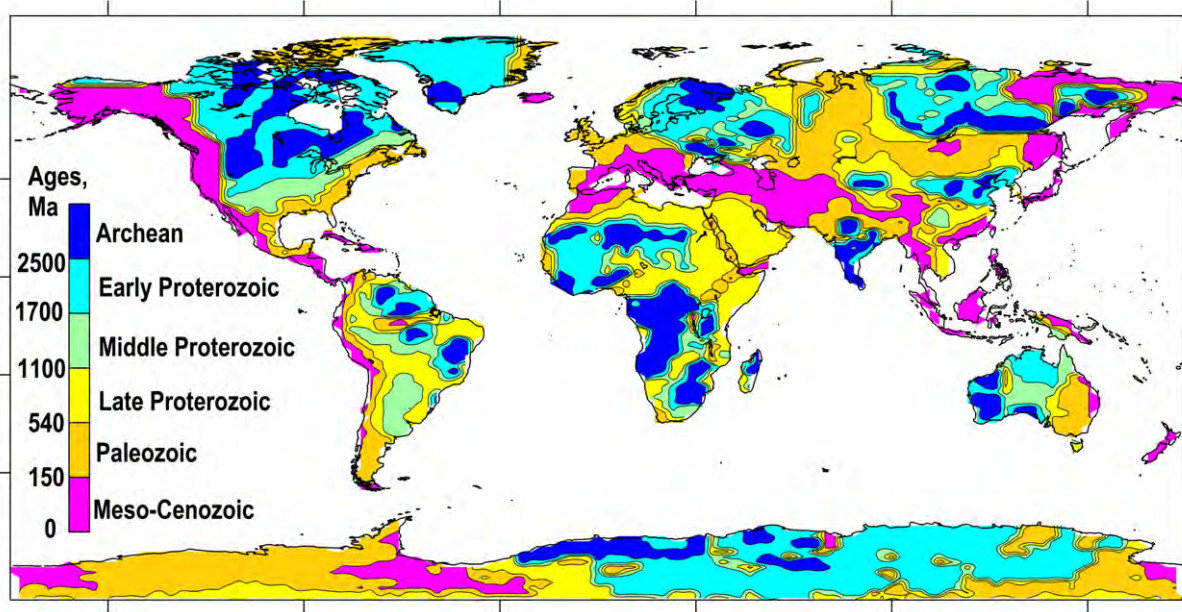


Fig. 3. Tectono-thermal age of the continental lithosphere based on a global $1^\circ \times 1^\circ$ model TC1 (modified after Artemieva, 2006). Since black and white image puts certain limitations on data presentation, for simplicity the map shows only six major geological epochs.

approximates heat flow at the base of the crust, i.e. the non-radiogenic component of surface heat flow (Lachenbruch, 1970).

There is an on-going debate on the relative contributions of crustal and mantle heat flow into the observed variations in surface heat flow of stable continents. Two end-member models of the thermal regime of the lithosphere attribute heat flow variations primarily (1) to variations in crustal heat production or (2) to lithospheric thickness variations (and thereby mantle heat flow variations). Regional studies indicate that either one or the other mechanism can dominate in different Precambrian cratons. Jaupart and Mareschal (1999) argue that surface heat flow variations in the Superior Province of the Canadian Shield are produced by lateral heterogeneity in the distribution of heat-producing elements within the crust. Indeed, the Superior Province is made of a large number of small (sometimes less than 50–100 km across) distinct crustal terranes, which amalgamated at 2.72–2.69 Ga. Strong crustal heterogeneity leads to significant lateral large-amplitude surface heat flow variations, which have a short wavelength (commonly less than 100 km), suggesting a crustal origin.

In North America, seismic data of the LITHOPROBE transects across the Canadian Shield indicate that the boundaries between the terranes are not vertical, and that within a 100–200 km wide zone along these boundaries the age of the crust and the underlying mantle can be significantly different. For example, at the eastern margin of the Canadian Shield, the middle Proterozoic crust of the Grenville province is underlain by the Archean mantle of the Superior province (Ludden and Hynes, 2000). It explains why in the Canadian Shield (and, in particular, at the Superior–Grenville boundary) mantle heat flow appears to have a uniform value across lithospheric terranes of different ages (Jaupart and Mareschal, 1999).

On the other hand, thermal models for South Africa cannot satisfy data from xenolith geotherms for the Archean Kaapvaal–Zimbabwe craton and the surrounding Proterozoic mobile belts if all surface heat flow variations are attributed entirely to variations in crustal radioactivity (Nyblade and Pollack, 1993). Therefore, variations in lithospheric thickness should be the principal factor controlling the surface heat flow pattern, providing basis for the hypothesis that thick cratonic lithosphere diverts heat sideways to the mobile belts (Ballard and Pollack, 1987).

Numerical models of mantle convection with floating continents (Lenardic and Moresi, 2001) resolve an apparent contradiction between two basic models of lithospheric thermal structure and demonstrate that they are the end-member solutions for layered and whole mantle convection models: the thermal resistance of the convecting mantle depends on the thickness of the upper thermal boundary layer, which in turn compensates the thermal resistance of the mantle. In case of the layered convection (i.e. thin convecting layer), the effect of lithospheric thickness on mantle heat flow is strong and large surface heat flow variations can be explained by small variations in relative lithospheric thickness. On the contrary, in case of whole mantle convection the dependence of mantle heat flow on lithospheric thickness becomes weak.

Thus, practical approaches to calculate lithospheric geotherms should account for both lateral variations in the bulk crustal heat production and in mantle heat flow (lithospheric thickness). Large uncertainty in the values of thermal parameters in the lithosphere results in non-uniqueness of numerical solutions: a large set of conductive geotherms can be produced for any surface heat flow value, complicating the “geophysically-meaningful” solution to the problem. Despite significant number of regional geothermal models published over the past 40 years, they are of a little use for global analysis since they are based on significantly different assumptions and do not permit any comparison between different tectonic provinces. By the turn of the millennium, the only existing global thermal model for the continental lithosphere was still the one published by Pollack and Chapman (1977). Their calculations were based on global-scale assumptions on thermal conductivity and radioactive heat production and were constrained only by surface heat flow values. In particular, the model was based on the assumption (constrained by 9 data points only) that, globally, $D = 8$ km and that 40% of surface heat flow is generated in the D -layer, with the remaining 60% coming from below (due to mid-lower crustal radioactivity, mantle radioactivity, and heat flow from the mantle). As a result, a family of conductive geotherms was calculated for the continental lithosphere; it provides a global “reference frame” still widely used, in particular in interpretations of xenolith P – T arrays.

A new global thermal model of the continental lithosphere (Artemieva and Mooney, 2001), based on the updated compilation

of Pollack et al. (1993) of surface heat flow measurements, took into account lateral variations in geological and tectonic structure of the crust. Data on the crustal structure combined with laboratory measurements of heat production in crustal rocks along exposed crustal cross-sections, as well as with petrologic constraints on the total crustal heat production, were used to calculate continental geotherms in the regions with high-quality heat flow data and steady-state thermal regime (Fig. 4). For these regions, the lateral resolution is primarily controlled by the wavelength of heat flow anomalies and the lateral resolution of the crustal seismic data. In particular, short wavelength anomalies in regions with highly heterogeneous heat flow were filtered to remove the crustal effect (e.g. produced by strong lateral variations in crustal thermal properties), resulting in lateral resolution of ca. 100 km. For regions of active tectonics with the transient thermal regime, lithospheric geotherms were based on non-steady state regional models and on xenolith P - T arrays. Sensitivity tests demonstrated that the overall resolution of the thermal model is ca. ± 50 °C at 100 km depth and ca. 25% for the lithospheric thermal thickness (Artemieva and Mooney, 2001). Although uncertainty in the values of thermal properties of the upper mantle can lead to a systematic bias of the model results, the model permits meaningful comparison of lithospheric geotherms for different continental structures. Since high-quality heat flow measurements cover less than 50% of the continents, the statistical relationship between the thermal regime of the continental lithospheric mantle and its tectono-thermal age has been used to fill in the “white spots” and to constrain

a global thermal model for the continents (Artemieva, 2006) (Fig. 5a). However, all results and conclusions of the present study are based solely on the thermal model constrained by borehole heat flow measurements (Artemieva and Mooney, 2001).

3.2. Structure of the CLM from seismic tomography models

The last two decades showed an astonishing progress in developing high-resolution global and regional seismic tomography models. The models show a general agreement, although the amplitudes and small-scale shapes of velocity anomalies can vary significantly from model to model (Ritzwoller and Lavelly, 1995). Given that the present study aims at examining global trends in the structure of the continental lithospheric mantle, further analysis is based on two recent global tomography models: (i) a global surface-wave tomography model of Shapiro and Ritzwoller (2002), further referred to as RW-SR and (ii) a global teleseismic body-wave V_s tomography model of Grand (2002), further referred to as BW-G. Since anelasticity leads to a strong non-linear dependence of seismic velocities on temperature, especially at high homologous temperatures, knowledge of absolute velocities in the mantle is needed to distinguish a non-temperature part in seismic tomography models. This requirement favors the use of the global surface-wave tomography model of Shapiro and Ritzwoller (2002), which gives absolute seismic velocities in the upper 250 km of the mantle (due to a near-surface sub-horizontal wave propagation, surface-wave models, in particular based on fundamental modes, lose resolution below this depth).

The surface-wave tomography model RW-SR is based on fundamental mode surface-wave group and phase velocities (Rayleigh group velocity at 16–200 s, Love group velocity at 16–150 s, and Rayleigh and Love phase velocity at 40–150 s) and is radially anisotropic in the upper 200 km of the mantle (Shapiro and Ritzwoller, 2002). Since seismic velocities are calculated by an over-parameterized Monte-Carlo inversion, the uncertainties in the results are difficult to assess. Given that propagation of surface waves is very sensitive to the crustal structure, seismic velocities in the surface-wave tomography model are best resolved at depths 100–200 km. The lateral resolution of the model, although calculated on a $2^\circ \times 2^\circ$ grid, probably does not exceed 500–1000 km. However, a comparison of the RW-SR model for regions where high-resolution regional surface-wave tomography models exist (e.g. van der Lee, 2002) shows that the model has a comparable lateral resolution for the lithospheric mantle.

The teleseismic body-wave V_s tomography model BW-G (Grand, 2002) is constrained in relative velocities and for the purposes of the present study is converted to the absolute velocities. The lateral resolution of the BW-G model is higher than the resolution of the RW-SR model since waves from distant earthquakes arrive to the receivers near-vertically and reflect the mantle structure beneath the receiver. However, a near-vertical wave propagation of teleseismic body-waves results in a vertical smearing of seismic velocities and, as a result, in a lower vertical resolution than for the surface waves model. Furthermore, smoothing regularizations, commonly used to compensate for an underdetermined posing of the inversion, complicate a quantitative comparison between the amplitudes of V_s velocity anomalies in the surface-wave and body-wave models.

Fig. 5b,c show lateral variations in the thickness of the continental lithosphere for the RW-SR and BW-G models, defined by a $2.0 \pm 0.5\%$ velocity anomaly relative to global continental reference velocity model IASP91 (Kennett and Engdahl, 1991). The range of $2.0 \pm 0.5\%$ in a velocity anomaly associated with the base of the seismic lithosphere (instead of a 2.0% anomaly sharp) was chosen to compensate for uncertainties in the seismic tomography models. Similar to the map of the thickness of the thermal lithosphere (Fig. 5a), the thickness of the seismic lithosphere is strongly correlated with surface tectonics and with tectono-thermal ages. Regions with thick seismic lithosphere have thick thermal lithosphere, associated with low lithospheric

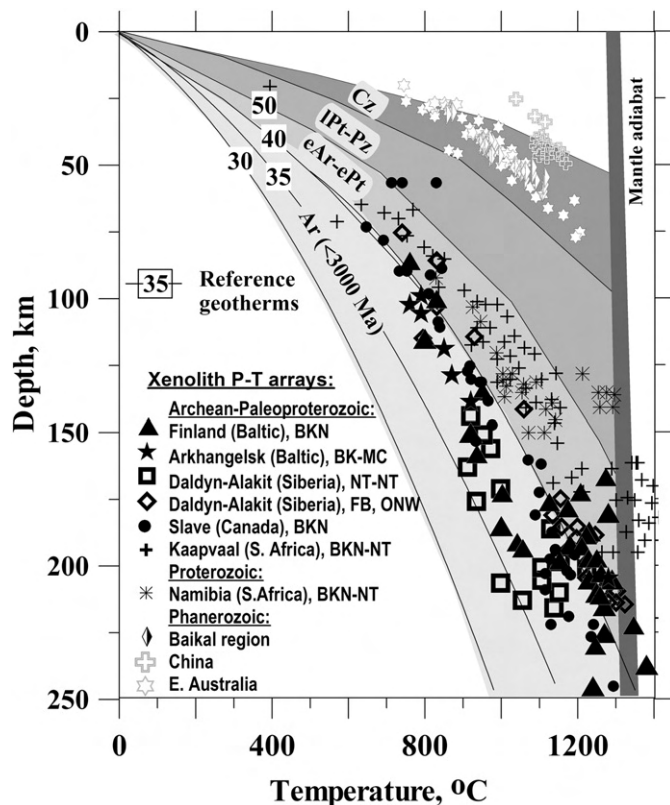


Fig. 4. Lithospheric geotherms for continental regions (modified from Artemieva, 2006). Thin lines – conductive geotherms of Pollack and Chapman (1977), values are surface heat flow in mW/m^2 . Lithosphere geotherms fall between reference geotherms of 30 and 40 mW/m^2 for Neoproterozoic; between 40 and 50 mW/m^2 for Paleoproterozoic and Neoproterozoic; between 50 and 65 mW/m^2 for Paleoproterozoic–Paleozoic and above 70 mW/m^2 for Cenozoic structures. Reworked Archean terranes have geotherms intermediate between Neoproterozoic and Paleoproterozoic structures. Xenolith P - T arrays from different continental locations are shown for comparison (see references in Artemieva, 2006). Abbreviations refer to different geothermobarometers (BKN=Brey et al., 1991; NT=Nimis and Taylor, 2000; MC=MacGregor, 1974; FB=Finnerty and Boyd, 1987; ONW=O'Neill and Wood, 1979).

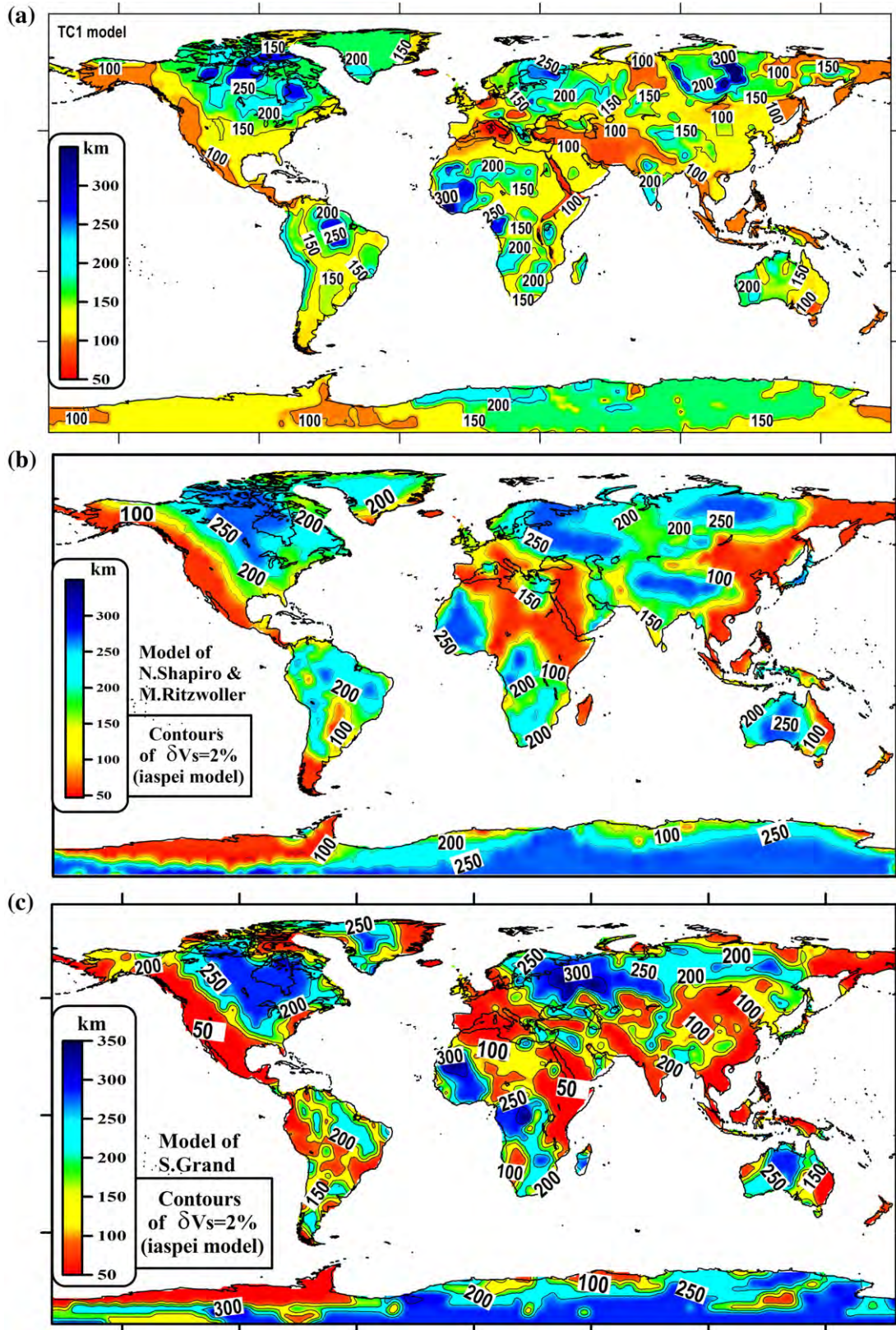


Fig. 5. Thickness of the continental lithosphere as defined from: (a) thermal modeling complemented by global statistical data on mantle temperatures (modified after Artemieva, 2006), (b) surface-wave seismic tomography (based on the model of Shapiro and Ritzwoller, 2002), (c) body-wave seismic tomography (based on the model of Grand, 2002), (d) correlation between thickness of seismic lithosphere (c) and thickness of thermal lithosphere (a) for the continents (excluding off-shore areas and Antarctica) calculated on a $5^\circ \times 5^\circ$ grid to account for different lateral resolution of the models and with the depth averaging of 75 km for seismic model and 50 km for thermal model to account for the depth uncertainty of the models. For seismic tomography models (oceanic regions are blanked), the lithospheric base is defined here as the depth where V_s velocity in the upper mantle is $2.0 \pm 0.5\%$ higher (to account for model resolution) as compared to the global continental velocity model *iaspei91*. Color version of the figure is available on-line.

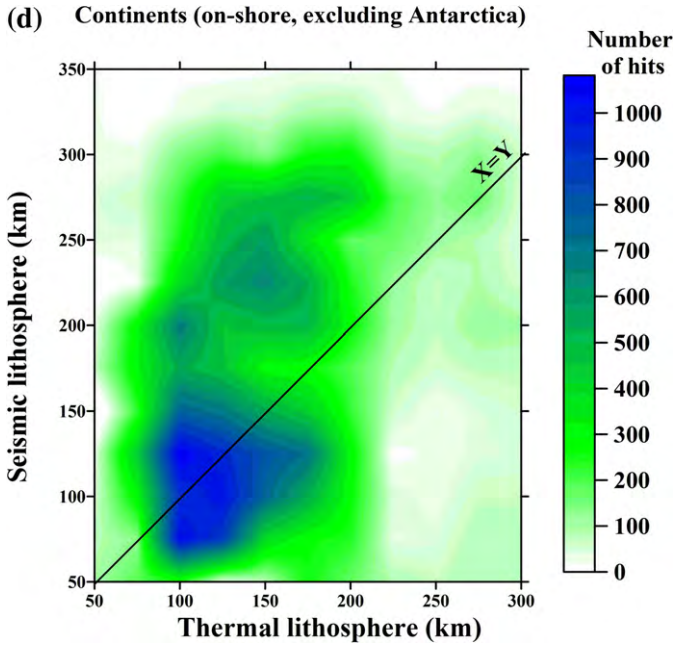


Fig. 5 (continued).

temperatures (Fig. 5a). The thickest lithosphere (in excess of 200 km) is restricted chiefly to the Precambrian cratons. Some cratonic regions, however, do not show strong positive velocity anomalies in the upper mantle either because they are not resolved (due to their small size, as the Indian and Tanzanian cratons, or due to an insufficient ray-path coverage, as the Western Australian cratons) or because they have lost deep lithospheric roots (e.g. the Sino-Korean craton (Menzies et al., 1993)). Some non-cratonic regions that show strong linear zones of

positive velocity anomalies in the upper mantle are associated with modern subduction zones (e.g. Hellenic arc, Tibet, Andes, Japan) which have cold temperatures within the slabs. These factors, together with different lateral and depth resolution of seismic tomography and thermal models result in a non-unique relationship between the thicknesses of seismic and thermal lithospheres (Fig. 5d).

4. Compositional heterogeneity of the CLM

4.1. Petrologic evidence

A substantial part of the present knowledge on the composition of the continental upper mantle is based on geochemical studies of abundant mantle-derived xenoliths, which provide a direct, although non-uniform and not necessarily representative (Artemieva, 2007), sampling of the upper mantle. Analyses of major-element compositions of oceanic peridotites and mantle-derived xenoliths from different tectonic settings indicate fundamental variations in composition of the lithospheric mantle (Boyd, 1989). A pronounced correlation between the age of the overlying crust and mantle chemical composition is interpreted as a secular, irreversible trend from highly depleted (due to loss of Fe and Al during melt extraction) Archean continental lithospheric mantle through intermediate Proterozoic mantle to fertile Phanerozoic continental and suboceanic mantle (Griffin et al., 1998). The depleted (low Fe, low Ca and Al, and low Ca/Al) composition of Precambrian lithospheric mantle is quantified by the iron content in mantle olivine ($mg\# = Mg/[Mg+Fe]$) or forsterite content ($Fo = 100 \cdot Mg/[Mg+Fe]$) which systematically increases from $Fo = 92\text{--}94$ in typical Archean lithospheric mantle through $Fo = 91.5\text{--}92.5$ in Proterozoic CLM to $Fo = 90$ in Phanerozoic CLM (Gaul et al., 2000) (Table 1, Fig. 6a). However, a secular trend of decreasing mantle depletion from Archean to Phanerozoic does not hold globally since in some Archean cratons (the Wyoming, Tanzanian and the Sino-Korean cratons) the lower part of the lithospheric mantle

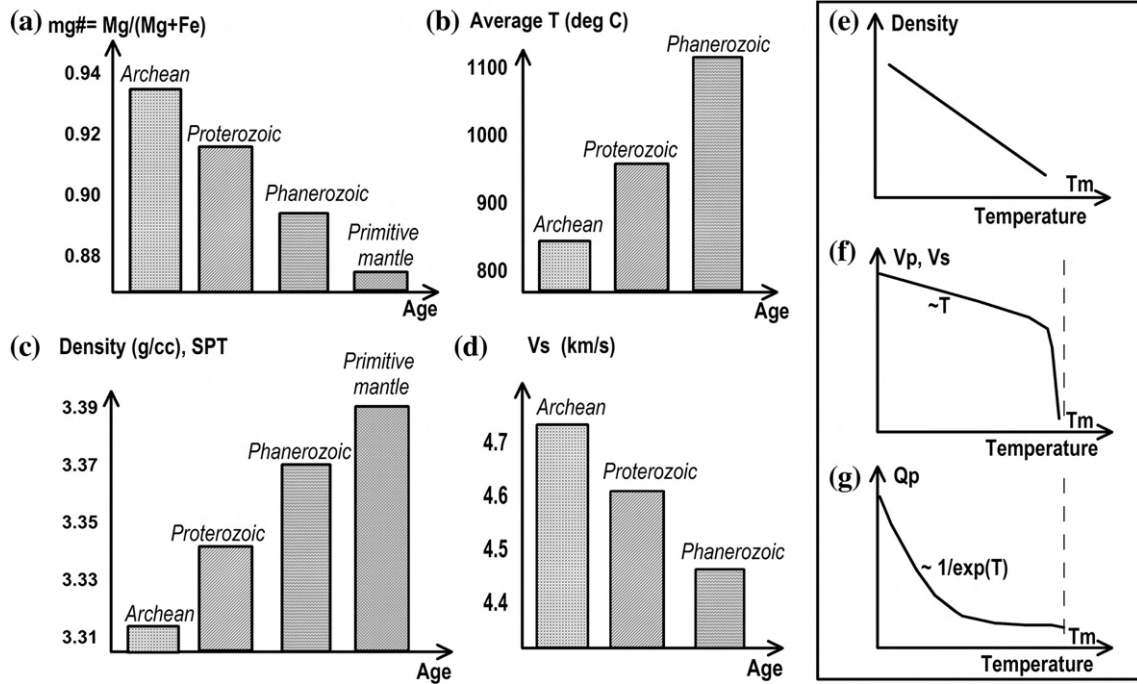


Fig. 6. Secular variations in average physical properties of the continental lithospheric mantle (CLM) due to compositional and temperature variations: (a) forsterite content, (b) average temperature in the CLM, (c) density at standard, i.e. room, P - T conditions, (d) S -wave seismic velocity. Primitive mantle (of pyrolite composition) is shown for a comparison. Right column illustrates the effect of temperature on: (e) density, (f) seismic velocities (e.g. Sato et al., 1989; Jackson et al., 1990), and (g) inverse seismic attenuation (e.g. Jackson, 2000). For example, a 4% Fe-depletion or a 100–150 °C temperature decrease in the mantle both cause a 1% increase in seismic velocity (Nolet and Zielhuis, 1994; Deschamps et al., 2002), while at *in situ* upper mantle temperatures, density of CLM of different ages can be similar, ca. 3.24 g/cc (Jordan, 1988). T_m – solidus temperature. (a), (c), (d) are based on xenolith studies of mantle peridotites (e.g. Hawkesworth et al., 1990; Pearson et al., 1995; Griffin et al., 1998; Boyd et al., 1999; Lee and Rudnick, 1999; Gaul et al., 2000; Lee, 2003).

has been effectively replaced by fertile mantle (or refertilized by infiltration of iron-rich basaltic melts) during Phanerozoic tectonic activity (Lee and Rudnick, 1999; Fan et al., 2000).

Compositional variations in lithospheric mantle, and primarily in iron-content, are reflected in densities and seismic velocities as measured in laboratory (Boyd and McCallister, 1976; Jordan, 1979; Jackson et al., 1990; Lee, 2003) and calculated for mean and end-member compositions of CLM based on mantle-derived peridotites (Griffin et al., 1998; Boyd et al., 1999; Gaul et al., 2000). While the density of lithospheric mantle systematically increases with age (from $3.31 \pm 0.02 \text{ g/cm}^3$ in Archean terranes, through $3.33\text{--}3.35 \pm 0.02 \text{ g/cm}^3$ in Proterozoic terranes, to $3.36\text{--}3.37 \pm 0.02 \text{ g/cm}^3$ in Phanerozoic terranes and to $3.38\text{--}3.39 \text{ g/cm}^3$ for primitive mantle of pyrolite composition), seismic velocities decrease with age from $V_s=4.37 \text{ km/s}$ in typical Archean lithospheric mantle to $V_s=4.24 \text{ km/s}$ in Phanerozoic lithospheric mantle (at $T=1000 \text{ }^\circ\text{C}$) (Table 1, Fig. 6c, d). A strong correlation between mantle density and elastic parameters and the age of the continental lithospheric mantle should be reflected in global seismic tomography and gravity models, showing a correlation with tectonic settings. Indeed, a joint inversion of global tomography model S16RLBM (Trampert and Woodhouse, 1995) and gravity data for petrologic models with variable content of iron and olivine indicates that temperature and iron anomalies beneath the continents are well correlated with surface tectonics down to ca. 300 km depth (Deschamps et al., 2002).

4.2. Geophysical evidence

Systematic variations in density and elastic parameters in continental lithospheric mantle caused by large-scale compositional heterogeneities should be reflected in global seismic tomography and gravity models. However, strong lateral variations in the thermal regime of the continental lithospheric mantle, and the strong effects of temperature variations on physical properties of the upper mantle rocks (e.g. Murase and Kushiro, 1979; Sato et al., 1989; Karato, 1993; Faul and Jackson, 2005), complicate interpretations of large-scale geophysical models in terms of compositional variations in the mantle: while iron-depletion systematically increases with age, mantle temperatures (at the same depth within the lithospheric mantle) show the opposite trend (Fig. 6a,b). The age-dependent variation in mantle temperatures will result in a density decrease in Phanerozoic regions due to thermal expansion (Fig. 6e), thus reducing the density contrast between depleted cratonic CLM and young fertile CLM (Fig. 6c). In contrast, the temperature increase results in a reduction of seismic velocity (Fig. 6f); thus a difference in mantle temperatures between Archean and Phanerozoic terranes will enhance velocity contrast between depleted and fertile mantles (Fig. 6d) supporting a common interpretation of seismic velocity anomalies in terms of “cold” versus “hot” regions and a conclusion that mantle velocities reflect chiefly temperature anomalies rather than variations in composition. Since the temperature difference between Archean and Phanerozoic terranes is maximal in the uppermost lithosphere (where it reaches $700\text{--}800 \text{ }^\circ\text{C}$ at 50–100 km depths) and gradually decreases with depth while a geotherm approaches the mantle adiabat, the “masking” effect of lateral temperature variations on mantle density anomalies and their “enhancing” effect on seismic velocity anomalies should be the strongest in the upper parts of the lithosphere.

The relative contribution of compositional and non-compositional (i.e. primarily, thermal) variations in the continental lithospheric mantle to gravity and seismic anomalies is the subject of an on-going debate (e.g. Forte and Perry, 2000; Röhm et al., 2000; Deschamps et al., 2002; Kaban et al., 2003; Perry et al., 2003; Artemieva et al., 2004; Godey et al., 2004). Griffin et al. (1998) argue that compositional anomalies can account for at least 50% of velocity anomalies observed in seismic tomography models. This conclusion is in accord with the

results of a recent global analysis of correlations between seismic elastic and anelastic anomalies constrained by Rayleigh waves and thermal anomalies in the upper 150 km of the mantle, which suggest that temperature variations alone can explain seismic V_s only in ca. 50% of continental regions (Artemieva et al., 2004). Furthermore, recent petrologic studies of the styles of continental rifting fail to explain lateral variations in rift-associated magmatism solely by variations in mantle temperature and require lateral variations in mantle depletion (Lizarralde et al., 2007).

Studies of the ratio between relative density and relative S-wave velocity anomalies in the mantle [$\zeta = \partial \ln \rho / \partial \ln V_s$] based on an inversion of gravity data and seismic tomography models further contribute to the debate on lateral and vertical compositional heterogeneity of the CLM (e.g. Forte et al., 1994; Forte and Perry, 2000; Deschamps et al., 2002; Perry et al., 2003; van Gerven et al., 2004). Factor ζ provides a crude diagnostic of the origin (thermal versus compositional) of density and velocity anomalies in the mantle: $\zeta > 0$ for purely thermal anomalies since temperature variations produce density and velocity variations of the same sign. The value of ζ in the real upper mantle is not well constrained. An influence of compositional variations on ζ factor is complicated and both cases, $\zeta > 0$ or $\zeta < 0$, are possible, depending on composition: synthetic ζ values calculated for two end-member upper mantle compositions give $\zeta > 0$ for olivine-garnet and $\zeta < 0$ for olivine-diopside mineralogies (Deschamps et al., 2002). The reported ζ values based on inversions of gravity and tomographic models are limited since many studies used low-degree spherical harmonics sensitive to the structure of the deep mantle. Joint inversions for the whole mantle, using degrees $l=2\text{--}8$ of spherical harmonics, gives $-0.3 < \zeta < 0.3$ with the change of the sign at ca. 300 km depth (Forte et al., 1994); the inversions for $l=11\text{--}16$ give $-0.05 < \zeta < 0.05$ for the upper 400 km with the change of the sign at ca. 220–240 km depth (Deschamps et al., 2002). Furthermore, negative ζ values between 75 km and 150 km depth and near-zero ζ values down to 220–300 km depth beneath the Proterozoic Central Australia suggest strong compositional variations in the cratonic upper mantle (van Gerven et al., 2004). However, the shapes of the curves for ζ and relative V_s anomaly variations with depth are significantly different, indicating that compositional anomalies with an intermediate length scale are important in the uppermost part of the CLM (Deschamps et al., 2002). The change of ζ sign at the depths where temperatures in the CLM are close to the mantle adiabat and thus thermal effect on velocity and density variations decreases, has been interpreted as indicating that the magnitude of mantle compositional anomalies progressively increases with depth (Deschamps et al., 2002).

These results indicate that, while lithospheric temperature plays the dominant role in controlling density and seismic velocity anomalies in the mantle, compositional variations as well as other effects play a significant role in determining lateral and vertical variations of seismic velocities and densities. Thus the question is how non-thermal (presumably, compositional) variations in lithospheric mantle can be distinguished from thermal anomalies in global seismic tomography (and gravity) models. Data on the thermal regime of stable continental lithosphere provides an exceptional opportunity to separate thermal and non-thermal effects in global geophysical models by subtracting the temperature-component from global observations. Such an approach, applied to an analysis of global elastic and anelastic seismic Rayleigh-wave tomography data, has demonstrated that for ca. 50% of the continents about one half of the amplitude of seismic velocity and seismic attenuation variations observed at a 100 km depth cannot be explained by temperature variations alone (Artemieva et al., 2004). A similar approach based on a global scale joint interpretation of gravity and thermal data has demonstrated significant density heterogeneity in the cratonic lithospheric mantle, even for the cratons of similar ages (Kaban et al., 2003).

This study extends this analysis to examine how seismic velocity variations of non-thermal origin change laterally and vertically in the continental lithospheric mantle. The approach is inspired by petrologic data on mantle xenoliths, which indicate a strong vertical compositional stratification in the lithospheric mantle of many Precambrian cratons with a downward increase in fertility (i.e. primarily in iron-content), which should lead to an STP velocity decrease with depth (e.g. Griffin et al., 1998; Lee and Rudnick, 1999; Lee, 2003; James et al., 2004).

5. Evaluating compositional anomalies in the CLM

5.1. Thermal contribution to seismic velocity anomalies

5.1.1. The method

Compositional (non-thermal) variations in the continental lithospheric mantle can be distinguished from seismic velocities if the effect of temperature variations is removed. Here, seismic velocity variations in the continental lithospheric mantle of a non-thermal origin are calculated as the difference between seismic velocities observed in tomography models and synthetic velocities, calculated from mantle temperatures with no a priori assumptions on compositional variations in the mantle or on presence of melts or fluids. The calculation of synthetic velocities $V_s^T(T, z)$ for the CLM is based on lithospheric geotherms constrained by borehole heat flow measurements (Artemieva and Mooney, 2001). Following the approach of Artemieva et al. (2004) and using experimental data on direct measurements of temperature-dependence of seismic velocities in mantle rocks and rock-forming minerals (e.g. Kampfmann and Berckhemer, 1985; Sato et al., 1989; Jackson et al., 1990; Lee, 2003; Matsukage et al., 2005), lithospheric temperatures are converted to seismic velocities. First, the elastic part of velocity anomalies is calculated as a velocity anomaly caused by the deflection of the regional geotherm from a typical continental geotherm of 50–55 mW/m² and assuming a linear dependence of velocity on temperature with a value of $\partial V_s / \partial T = 0.35$ m/s/K commonly accepted for olivine, which is the predominant mineral in the upper mantle (>60%) (Sumino and Anderson, 1982). The choice of the same value of $\partial V_s / \partial T$ globally implies that no a priori assumptions are made on lateral or vertical compositional variations in the lithospheric mantle. A systematic shift of the calculated values would be possible if the remaining <40% of mantle constituents were significantly altering the olivine value of $\partial V_s / \partial T$ (the author is unaware of any laboratory studies addressing this question). Then, the elastic part of synthetic velocities $V_s^T(\text{elastic})$ is calculated by adding a temperature-induced velocity variation to the global continental reference velocity model *ak135* (Kennett et al., 1995).

Since at seismic frequencies anelasticity has an important effect on seismic velocities (Karato, 1993), the anelastic correction is calculated as (Minster and Anderson, 1981):

$$V_s^T = V_s^T(\text{elastic}) \left[1 - CQ^{-1}(\tau, P, T) \right],$$

where $C = 2/\tan(\pi\alpha/2)$ and $Q^{-1} = A\tau^\alpha \exp(-\alpha E^*/RT)$ (Jackson et al., 1992). Assuming that for the upper mantle velocities $Q_p = 2.25 Q_s$ (e.g., Anderson et al., 1965), P-wave attenuation is converted to S-wave attenuation. Here E^* is the activation energy ($E^* = 560$ kJ/mol at $z = 100$ km), R is the gas constant, T is temperature, τ is the oscillation period, A is a scaling constant (following Sobolev et al. (1996), $A = 0.148$), and the exponent α (typically $\alpha \sim 0.15$ – 0.30) is determined from seismic studies and laboratory measurements on the upper mantle rocks (Jackson et al., 1992). The calculations of synthetic velocities $V_s^T(T, z)$ are made for frequency of 40 s, consistent with the seismic frequency of the surface-wave tomography model. The difference ΔV_s between the calculated synthetic velocities $V_s^T(T, z)$ and seismic velocities observed in tomography models is calibrated at each depth with respect to the reference velocity model *ak135* (Kennett et al., 1995); it shows the

contributions of non-thermal effects to anomalies of seismic velocity in the continental lithospheric mantle.

5.1.2. Uncertainties in the amplitudes of the anomalies

Given an uncertainty in the scaling parameters, in particular for the anelastic correction, the non-uniqueness of seismic inversions (e.g. Montagner and Kennett, 1996) and the uncertainty in thermal properties, in particular of the lithospheric mantle (see Artemieva and Mooney (2001) for discussion), a systematic shift in the calculated amplitudes of non-thermal velocity anomalies cannot be ruled out.

(1) Uncertainties associated with seismic tomography models.

- Surface wave tomography model is highly sensitive to the crustal correction, in particular in the upper 100 km. It may result in artifact anomalies in regions with poorly known crustal structure (Bassin et al., 2000).
- Use of overparameterized Monte-Carlo inversion in the surface wave model makes it difficult to estimate the model uncertainty, in particular the uncertainty in the amplitudes of the velocity anomalies.
- In the body wave tomography model, velocity amplitudes are significantly lower than in the surface wave tomography model due to a near-vertical wave propagation in the uppermost mantle, which leads to a vertical “smearing” of the signal and “averaging” of amplitudes over a large depth window.
- The type of damping used in seismic inversion (e.g. smoothing of the amplitudes or of the gradients of velocity anomalies) has a strong effect on the amplitudes of velocity anomalies (see Section 3.2).

(2) Uncertainties associated with thermal and synthetic velocity models.

A systematic shift in the amplitudes of synthetic velocity anomalies $V_s^T(T, z)$, and thus in the amplitudes of non-thermal anomalies, is possible due to:

- the assumption of olivine value of $\partial V_s / \partial T$ for calculation of the elastic correction,
- the uncertainty in scaling parameters for the anelastic correction,
- a systematic shift in mantle temperatures due to unknown thermal properties of the lithospheric mantle (see Section 3.1),
- the choice of a typical continental (Paleozoic) geotherm of 50–55 mW/m² as the reference thermal model for the continental lithosphere.

Specifically, the sensitivity analysis shows that a 100 °C shift in mantle temperatures (which is about the accuracy of the thermal model for the lithospheric mantle, Artemieva and Mooney, 2001) may lead to a ca. 0.8% change in the values of non-thermal velocity anomalies. Choice of a Cenozoic or an Archean geotherm as the reference model will shift the amplitude of synthetic velocity anomalies by 1–2% in the shallow parts of the lithosphere with a smaller effect in its lower part, where a lithospheric geotherm approaches mantle adiabat. In both cases, uncertainties associated with the thermal model are significantly smaller than the range of seismic velocity variations in the tomography models and the calculated variations of ΔV_s .

Having in mind these limitations, the following discussion focuses largely on the qualitative comparison of different tectonic structures laterally and mantle chemical stratification vertically. First, the global patterns of composition-induced velocity anomalies and their possible origin are discussed, then the regional examples (lithosphere cross-sections) are provided for Europe, Australia, Asia, North America, and South Africa.

5.2. Global patterns of compositional velocity anomalies

Seismic velocity anomalies ΔV_s in the continental lithospheric mantle that cannot be explained by temperature variations alone

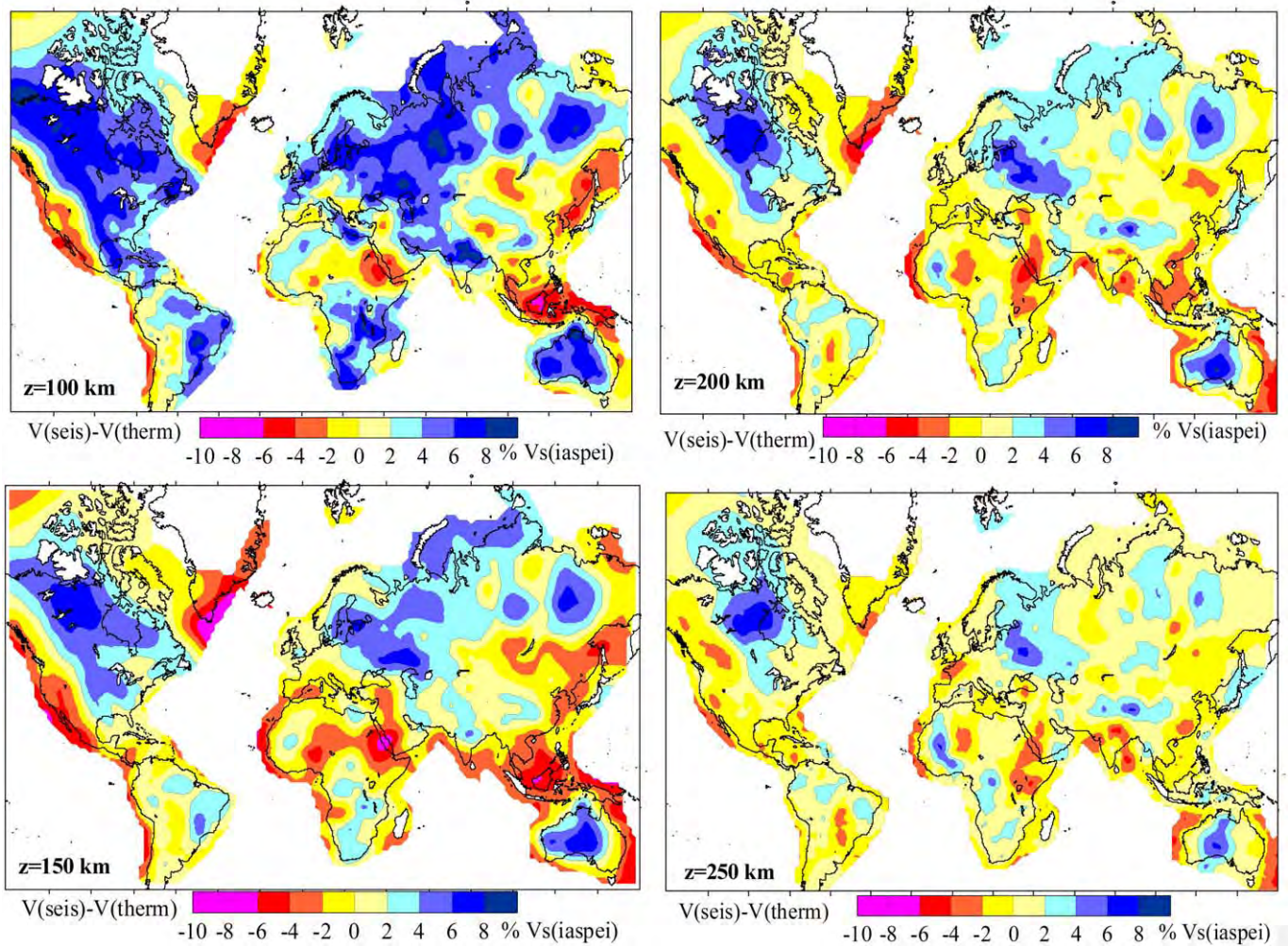


Fig. 7. Compositional (non-thermal) seismic velocity variations in the lithospheric mantle at depths of 100 km, 150 km, 200 km, and 250 km calculated as the difference between the observed seismic velocities (based on the surface-wave tomography model of Shapiro and Ritzwoller, 2002) and seismic velocity variations caused by temperature deflection from a typical continental geotherm of 50–55 mW/m².

(referred to hereafter as non-thermal anomalies) are based on the surface-wave tomography model RW-SR (Shapiro and Ritzwoller, 2002). The results (Fig. 7) are presented for four depths slices in the mantle: 100 ± 25 , 150 ± 25 , 200 ± 25 , and 250 ± 25 km. The thermal

model used to calculate the velocity anomalies of non-thermal origin was interpolated to the lateral resolution of the tomography model (500 km). Clearly, the results are more reliable for regions with a good coverage by borehole heat flow measurements (Fig. 8).

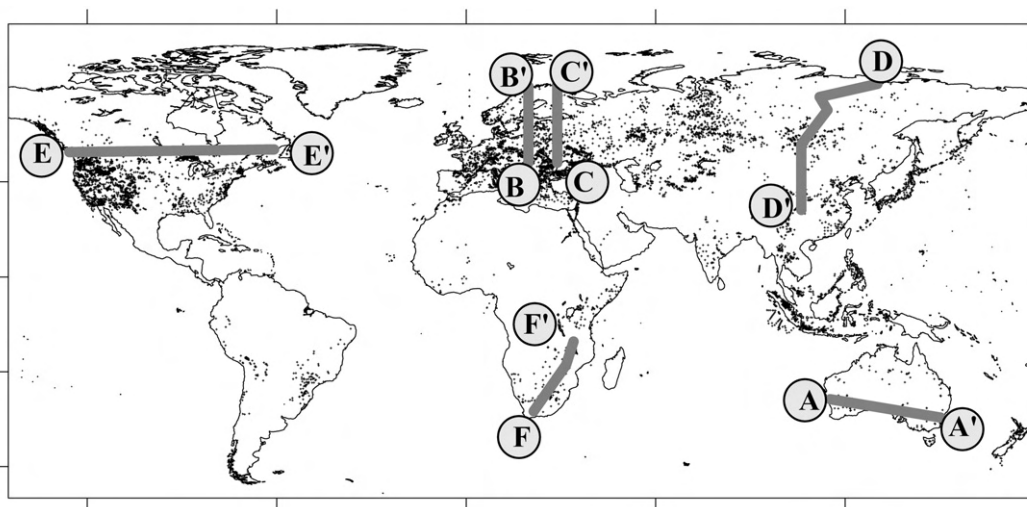


Fig. 8. Locations of the cross-sections shown in Figs. 9–13. The choice of the profiles was dictated by data coverage by surface heat flow measurements (shown by dots).

A large span in the amplitudes of the calculated anomalies (Fig. 7) results from large amplitudes of seismic velocity anomalies in the surface-wave tomography model RW–SR which range from ca. –5% to +9% (with respect to *iasp91*) at a 100 km depth and from ca. –3.5% to +7.5% at a 200 km depth. For a comparison, at 100 km depth the relative amplitudes of synthetic velocity anomalies $V_s^T(T, z)$ range from ca. –4% to +5% and typically contribute 25–75% to the total amplitude of the observed seismic velocity anomalies in the oldest parts of the continents. In tectonically active regions, the ratio of relative synthetic velocity anomalies to relative observed velocity anomalies may be significantly higher, in particular due to the presence of fluids and melts in the upper mantle, which have a strong effect on observed seismic velocities but are unaccounted in the synthetic velocity model $V_s^T(T, z)$.

Non-thermal velocity anomalies correlate strongly with surface tectonics (Fig. 7). At all depths, positive anomalies correlate with the cratons (Fig. 3). These velocity anomalies cannot be attributed to underestimation of mantle temperatures: temperatures 200–300 °C lower than in the thermal model (Artemieva and Mooney, 2001) are required to reduce the value of ΔV_s anomalies to zero. However, compositional anomalies due to iron-depletion can explain the misfit ΔV_s between seismic V_s and theoretical $V_s^T(T, z)$ in the cratonic lithosphere. The major deep-extending iron-depleted keels are observed in the Slave/Hearne cratons of the Canadian Shield, the western part of the East European Craton, the Siberian craton, and, to a lesser extent, in South Africa, the West African and Congo cratons. The strong anomaly in Central Australia may be misplaced from the Archean to Proterozoic terranes due to a poor ray-path coverage of Western Australia in the tomography model based on SKIPPY data (see e.g. Fig. 6 in Simons et al., 1999). An unexpected positive anomaly is observed at the eastern margin of the Siberian craton, in the region of intensive Cenozoic folding and the suspected plate boundary. Although this velocity anomaly can, in part, be attributed to an incomplete crustal correction in the tomography model for the region with no seismic data (mantle temperatures were assumed to be the same as in other Cenozoic fold belts), the presence of several Archean-early Proterozoic terranes further to the east (Fig. 3) suggests that some of the cratonic mantle could be trapped beneath the Verkhoyansk orogen. A sublittoral high velocity anomaly beneath the Tibet may reflect the depleted Archean lithosphere of the Indian plate, which can be traced down to at least a 250 km depth (Fig. 7).

It is worthy of note that the lateral extent of the areas with high velocity anomalies of non-thermal (most probably, compositional) origin diminishes with depth, so that at the greatest depth resolved by the tomography model (250 ± 25 km), high velocity anomalies are observed only within the internal parts of the cratons. If these anomalies are due to mantle depletion, the reduction of their lateral

size with depth may indicate either (a) a progressive growth or accretion of younger Proterozoic terrains onto highly depleted Archean nuclei or, alternatively, (b) a progressive enrichment inwards from the peripheries during a long-term interaction of depleted lithospheric keels with material from the convective mantle (e.g. metasomatism and erosion).

Negative non-thermal velocity anomalies are clearly correlated with continental regions of active tectonics such as modern orogens, areas of high lithosphere extension, and regions of modern intra-plate magmatism. The only exception from this pattern, a low velocity anomaly along the eastern coast of Greenland, can result from smearing of a strong off-shore low velocity anomaly around Iceland. In regions of active tectonics, high subsolidus temperatures, partial melts and/or fluids are the likely cause of ΔV_s anomalies. The next section (Tables 2, 3) summarizes the possible origins of seismic velocity variations in the continental lithospheric mantle, which cannot be explained by temperature variations alone.

5.3. Possible origin of non-thermal velocity variations in the upper mantle

5.3.1. Mantle composition and mineralogy

Three major upper mantle minerals are orthopyroxene, clinopyroxene, and garnet. Compared to olivine (for $X_{Fe}=0.1$), calcium-rich clinopyroxene has ca. 0.8% lower S-wave velocity and slightly lower density (Anderson and Isaak, 1995). For a hypothetical olivine-rich ($X_{Ol}=57\%$) end-member of the upper mantle composition, an increase in diopside content from 12% to 18% leads to a ca. 0.4% decrease of mantle S-velocity (Nolet and Zielhuis, 1994) and can cause some density decrease (Table 2).

Recent study of the effect of mantle mineralogy on seismic velocities in the upper mantle indicate that while chemical differentiation of the oceanic mantle can be described by one parameter (Mg#), the continental trend requires two parameters (Mg# and Opx#) to characterize seismic velocities and density of the continental peridotites (Matsukage et al., 2005). This principal difference between the oceanic and the continental trends is ascribed by the authors to the fact that compositional variations in oceanic peridotites are caused by one melting event, while in the continental mantle at least two processes (partial melting and the addition of Si-rich materials) control chemical compositions of peridotites. At low pressures (at 70 km to 190 km depth) seismic velocities are controlled by variations in orthopyroxene content. Deeper in the mantle, the effect of partial melting (and depletion) becomes dominating because of a strong pressure-dependence of V_s in orthopyroxene. While the range of Mg# variations in the CLM is 0.89 to 0.94, the range of Opx# variations spans from 0.06 to 0.45. An increase of Opx# by 0.2 at pressures

Table 2
Non-thermal effects on variations of upper mantle density and V_s seismic velocity

Parameter	Affected depth	$\delta\rho$	δV_s	Reference
Iron content increase	CLM	–1.4% (for $X_{Fe}=+4\%$)	+1.0% (for $X_{Fe}=+4\%$)	D02, L03
Garnet content increase	CLM	>0	>0	D02
Substitution of pyroxene-rich garnet by grossular garnet	CLM	<0, Weak effect	>0	D02
Clinopyroxene content increase	CLM	<0	–0.4% (for $X_{di}=+6\%$)	NZ94
Orthopyroxene content increase	CLM (70 to 190 km depth)	No effect	Up to –1.8%	M05
Fluids	CLM	Indirectly, through the effect on solidus	Indirectly, through the effect on solidus	T81
Anelasticity at high homologous temperature $T/T_m > 0.95$	The lower part of the TBL	No effect	–6%	S89
Melts	Chiefly the lower part of the TBL	<0	–10% for ~5% melt (strongly depends on melt geometry)	MK79
Anisotropy	CLM	No effect	Either sign	BIM98

Where absolute values are unavailable, the sign of δV_s and $\delta\rho$ variation is given. Positive values (>0) indicate a velocity or density increase, while negative values (<0) refer to a decrease in one of the parameters. See Section 5.3 of the discussion.

References: BIM98 – Ben Ismail and Mainprice, 1998; D02 – Deschamps et al., 2002; L03 – Lee, 2003; MK79 – Murase and Kushiro, 1979; M05 – Matsukage et al., 2005; NZ94 – Nolet and Zielhuis, 1994; S89 – Sato et al., 1989; T81 – Tozer, 1981.

Table 3
Tectonic settings with density and velocity anomalies (at SPT, thermal effect excluded) with respect to “normal” (Fo90) stable continental lithosphere (e.g. of Paleozoic platforms)

Tectonic setting	Major factors affecting ρ and V_s	$\delta\rho/\rho_o$ (%)	$\delta V_s/V_o$ (%)
Phanerozoic or metasomatised Fe-enriched cratonic mantle (Fo=90)	• If high garnet content	>0	>0
Proterozoic cratonic mantle	• If high diopside content	<0	-0.4%
Archean cratonic mantle	Intermediate Fo=92	-0.6–1.2%	+0.4%
Active continental regions (Plume-related)	Low Fe (Fo=93)	-1.8%	+1.3%
	• Melts	<0	-10% for ~5% melt
	• Subsolidus T	No effect	-6% (in a 10 km thick basal layer)
Subducted Precambrian slab=crust 40 km+110 km thick low-Fe (Fo92) mantle	• Composition of crust & mantle	-6.2% (Overall effect)	<0 (crust), +1% (mantle)
	• Metamorphism (in a 20 km thick layer),	+0.4% (Overall effect)	No effect
	• Fluids	No effect	<0
Subducted Phanerozoic slab=40 km crust+80 km thick harzburgite mantle (high ol, low gnt, no cpx)	• Composition of crust & mantle	-6.7% (Overall effect)	<0 (crust),
	• Metamorphism (in a 20 km thick layer),	+0.4% (Overall effect)	No effect (mantle)
	• Fluids	No effect	No effect
			<0
Orogens	• Metamorphism (in a 20 km thick layer)	+1.0% (Overall effect for 80 km thick mantle)	No effect
	• Fluids	No effect	<0
	• Melts?	<0	-10% for ~5% melt

See Section 5.3 of the text for references.

between 4 GPa and 7 GPa results in a ca. 1% decrease in V_s (Matsukage et al., 2005).

A decrease in Mg# by 4–5 units (which corresponds to a typical difference between Archean to Phanerozoic CLM) results in a 1% S-velocity decrease and in a ca. 1.4% density increase (Nolet and Zielhuis, 1994; Deschamps et al., 2002) and has the same effect on V_s as an increase of mantle temperature by 220 °C (Lee, 2003). Since metasomatic enrichment of depleted cratonic lithosphere by basaltic melt during intraplate magmatic events may result in an increase in iron (and garnet) content, and increase in Fe number, it produces similar changes in velocity and density, with the largest velocity and density changes in the lower parts of the lithosphere.

Garnet has both S-velocity and density significantly higher than olivine ($\delta V_s = +13\%$ and $\delta\rho = +7.3\%$ for grossular and $\delta V_s = +3.5\%$ and $\delta\rho = +10.5\%$ for pyrope-rich garnet) (Anderson and Isaak, 1995). Thus, an increase in garnet content in the mantle (e.g. $\delta X_{\text{gnt}} \sim 4\text{--}8\%$ from Archean to Phanerozoic mantle, Fig. 6a) significantly increases both density and S-wave velocity, while substituting pyrope-rich garnet for grossular garnet results in a velocity increase accompanied by a weak density decrease (Deschamps et al., 2002).

Thus, variations in iron, garnet, orthopyroxene, and clinopyroxene content in the upper mantle have different effects on the pair of two major parameters derived from geophysical surveys: bulk density and seismic velocity (Table 2). Combined inversion of gravity and seismic tomography model demonstrated that for all continental regions correlation between ρ and V_s (temperature variations present) does not exceed -0.4 at depths between 80 and 180 km and tends to zero above and below these depths (Deschamps et al., 2002).

5.3.2. Fluids

At depths greater than 100 km (i.e. beyond the dehydration depth of most hydrous minerals) the continental upper mantle is essentially dry: the amount of water does not exceed 0.03 wt.% of olivine (Karato and Wu, 1993; Hirth et al., 2000). However, at the sites of paleosubduction zones the amount of water in the mantle can increase by 3–10 times due to its downward transport and storage by dense hydrous magnesium silicates (Nolet and Zielhuis, 1994). A direct effect of the presence of such an amount of water in the mantle on seismic velocities and densities is negligible (Tozer, 1981). Volatiles, however, may have an indirect effect on velocities by affecting the solidus temperature T_m and causing anelastic behavior at high homologous temperature T/T_m , where the velocity–temperature relationship becomes strongly nonlinear (Fig. 6f, Murase and Kushiro, 1979; Karato, 1993). Experimental studies of seismic velocities (at ultrasonic frequencies) in dry peridotite at high T/T_m indicate that ca. 6% drop in V_p can be explained by subsolidus temperatures even with no melt being present (Sato et al., 1989). The effect of high

homologous temperature on shear velocities should be similar; however until melting starts, high subsolidus temperatures would have no effect on mantle density other than thermal expansion. Thus, seismic velocity and density can exhibit a significantly different temperature-induced behavior at the base of the TBL.

5.3.3. Melts

Although the presence of partial melts is a direct consequence of high mantle temperatures, it also implies a phase change and is considered here as a cause of non-thermal (i.e. phase-change related) velocity anomalies. The effect of melts on V_s velocities in anhydrous peridotite has been experimentally studied by Murase and Kushiro (1979), who found a dramatic increase of melt fraction at supersolidus temperatures leading to a dramatic decrease in velocity: ca. 5% of melt lead to more than a 10% velocity decrease. However, theoretical analysis indicates that the amount of melt even beneath the mid-ocean ridges is only ca. 2% (McKenzie, 1985). The amount of melt in the continental lithospheric mantle should be even smaller because interconnected melt is gravitationally unstable and migrates upwards even at concentrations of $\ll 1\%$ (McKenzie, 1989). Since the amount of melt in the upper mantle is poorly constrained and velocity depends dramatically on the geometry of melt distribution in the solid matrix (Faul, 1997) and on the wetting angle (low for aqueous fluids and high for CO_2 -rich fluids (Cmíral et al., 1998)), quantitative interpretations of velocity anomalies in the presence of melt remain rather speculative. Small pockets of melt in the mantle should not have a strong effect on bulk mantle density.

5.3.4. Other effects

Laboratory experiments on fine-grained olivine aggregate indicate that the subgrain size can critically affect seismic attenuation at near-solidus temperature (1200–1285 °C) (Gribb and Cooper, 1998). Since this effect is not incorporated in the calculated synthetic seismic velocities, a part of non-thermal velocity anomaly at the base of thermal can be attributed to anelastic effects related to changes in the grain size and grain boundary relaxation at high temperatures.

5.4. Regional examples of compositional variations in the CLM

5.4.1. Lateral and vertical model resolution

Figs. 9–13 provide regional examples of lateral and vertical variations of non-thermal seismic velocity anomalies. The profiles (their locations are shown in Fig. 8) show vertical cross-sections down to the depth of 250–300 km for the deflection of seismic tomography velocities from the synthetic velocity–depth profiles. The synthetic seismic velocity $V_s^T(T, z)$ in the lithospheric mantle has been calculated by introducing temperature corrections to the *ak135* model (Kennett

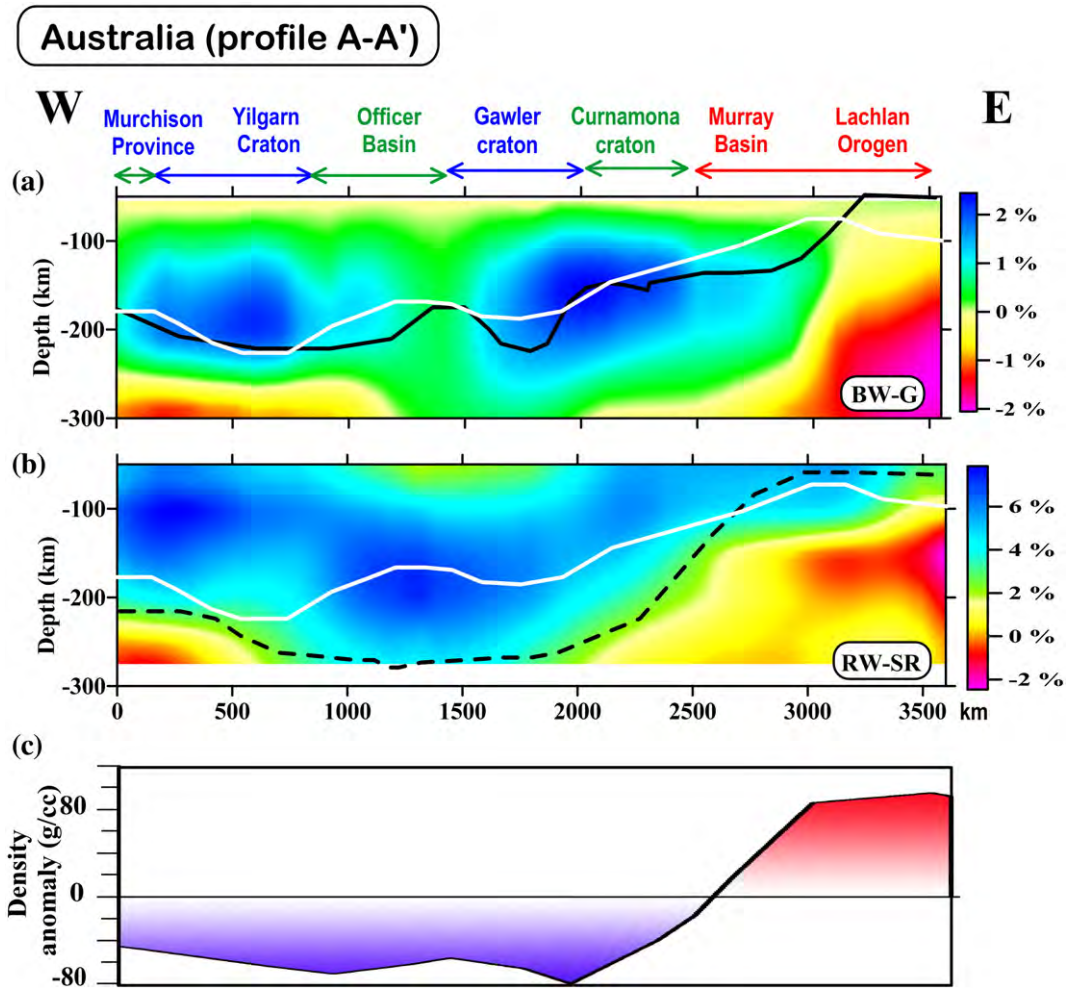


Fig. 9. (a, b) Compositional (non-thermal) seismic velocity variations in the lithospheric mantle across Australia (profile A-A' in Fig. 8) calculated as the difference between the observed seismic velocities and seismic velocity variations caused by temperature deflection from a typical continental geotherm of 50–55 mW/m². Seismic velocities are based on the surface-wave tomography models of Shapiro and Ritzwoller, 2002 and Grand, 2002. Black lines – lithospheric base as defined by a 2% δV_s anomaly with respect to *ak135* (Kennett et al., 1995) in the BW-G (solid line) and RW-SR (dashed line) tomography models; white lines – base of thermal lithosphere (defined by 1300 °C isotherm). Color lines on the top refer to the geological ages: blue – Archean-early Proterozoic, green – mid-late Proterozoic, red – Phanerozoic. (c) Density anomaly of non-thermal origin in the lithospheric mantle along the same profile (after Kaban et al., 2003). The plot shows density effect integrated over the entire thickness of the lithospheric mantle so that the depth distribution of density anomaly is unknown.

et al., 1995) to account for differences between the regional lithospheric geotherm and the average continental geotherm of 50–55 mW/m² (Fig. 9c). Thus, deflections of seismic velocities observed in tomography models from the reference velocity model *ak135* corrected for temperature variations in the CLM are of a non-thermal origin and are caused either by compositional heterogeneities in the CLM or by presence of fluids and/or melts. Clearly, data on lithospheric geotherms is an important input parameter for the modeling; thus the choice of the profiles was dictated by the areal coverage by surface heat flow measurements (Fig. 8).

While seismic tomography provides a “snapshot” of the present physical state of the CLM, surface heat flow measurements reflect the past thermal conditions in the mantle, with the time delay of the thermal anomaly being proportional to the squared depth of its origin, $\tau = z^2/\chi$, where χ is thermal diffusivity. It means that if the thermal model were constrained solely by borehole data, it would have been erroneous to compare seismic tomography anomalies with thermal regime of the lithosphere for continental regions with tectono-thermal ages younger than Carboniferous–Permian (see Section 3.1). For these continental regions the thermal regime of the lithosphere was constrained not by heat flow measurements, but primarily by xenolith data and transient thermal models (Artemieva and Mooney,

2001 and references therein), thus making a comparison of seismic and thermal models meaningful.

Regional examples of lateral and vertical variations of composition-induced seismic velocity anomalies are presented mainly for the surface-wave tomography model RW-SR (Shapiro and Ritzwoller, 2002). Due to a near-vertical wave propagation of teleseismic body-waves, velocity anomalies δV_s in the body-wave tomography model (Grand, 2002) are vertically smeared, leading to its low vertical resolution and much smaller amplitudes of velocity anomalies as compared to the surface wave model RW-SR. Small amplitudes of velocity anomalies in the body-wave model BW-G make it difficult to perform its quantitative comparison both with the RW-SR model and with mantle temperatures, despite a qualitative agreement of all three models. The discrepancy between the RW-SR and BW-G models is caused (a) by significant differences in wave propagation, which results in different lateral and vertical resolution of the RW-SR and BW-G models, and (b) by the principal differences in the inversion procedure for surface-wave and body-wave tomography models (see Section 3.2).

Low lateral resolution (ca. 500–1000 km) of the tomography model RW-SR puts certain limitations on interpretations of regional results. A global thermal model constrained by surface heat flow measurements

(Artemieva and Mooney, 2001) has an effective (slightly variable) lateral resolution in the range of 100–500 km in regions with heat flow measurements. This resolution is defined by borehole coverage and by filtering of short-wavelength (ca. 100 km) variations of surface heat flow caused by heterogeneities of thermal properties of the crust. To allow the direct comparison of seismic and thermal models, lateral resolution of the thermal model was reduced to 500 km by interpolation. The thermal model provides lithospheric temperatures at a shallow depth in the mantle with an accuracy of ± 50 °C which, in other words, if the temperature value is fixed, corresponds to a depth uncertainty of 15–20 km at a 100–200 km depth for a typical continental geotherm. The vertical resolution of the RW–SR model is ca. 50 km. Since the vertical resolution of the body-wave model BW–G is significantly weaker (not better than 75 km), the results are shown primarily for the RW–SR model. Note that the base of the seismic lithosphere shown in Fig. 5b, c was defined by $+2.0 \pm 0.5\%$ velocity anomaly relative to *iasp91*, while seismic LAB shown in Figs. 9–12 is based on a 2% anomaly sharp.

5.4.2. Australia

The sublatitudinal profile across Australia, from the Archean Yilgarn craton in the west to the Paleozoic Lachlan orogen in the east (A–A' in Fig. 8), reveals strong heterogeneity of the CLM beneath Australia (Fig. 9a,b). Velocity anomalies of non-thermal origin (indicative of compositional heterogeneity) strongly correlate with surface tectonics. A strong positive ΔV_s anomaly ($+4+6\%$ in the RW–SR model) persists down to 200–250 km depth below the Archean Yilgarn and Gawler cratons and below the Mesoproterozoic block between them. In the body-wave model BW–G, which has higher lateral resolution, the largest ΔV_s amplitudes (ca. 2%) are observed only beneath the Archean blocks, while the Proterozoic Officer Basin has significantly lower non-thermal velocity anomalies in the CLM. High ΔV_s in the cratonic lithospheric mantle are, most likely, caused by

iron-depletion (Tables 2, 3). However, due to a significant discrepancy in the amplitudes of ΔV_s anomalies calculated for BW–R and RW–SR models, the degree of this depletion is difficult to quantify. The west–east transition from depleted cratonic to non-cratonic fertile CLM is marked by a sharp (ca. 2%) change in ΔV_s . Gravity data strongly support the results of the present study (Kaban et al., 2003). Density anomaly in the lithospheric mantle (calculated from mantle residual gravity anomalies corrected for lateral temperature variations) is negative beneath the Precambrian part of the continent (and may be interpreted in terms of ca. 1.5% of mantle depletion) and becomes positive to the east from the Tasman Line (Fig. 9c). The Proterozoic Curnamona craton marks the edge of the Australian craton and the transition to fertile, thin, warm Phanerozoic lithosphere; however, the uppermost parts of the lithospheric mantle beneath the Murray Basin have high ΔV_s , and are likely to have composition similar to the cratonic.

The base of the strong compositional anomaly in the CLM can be interpreted as the base of petrologic lithosphere; it shallows eastwards towards the Proterozoic Curnamona Craton (Adelaide Syncline) and the Phanerozoic Murray Basin where the CBL is only 100–150 km thick (Fig. 9b). Beneath the Archean Gawler block the petrologic lithosphere persists down to at least 250 km depth. These results are in a general agreement with the joint seismic tomography-gravity inversion for Australia (van Greven et al., 2004). In the latter study, compositional anomalies are estimated to make a significant contribution to seismic velocity anomalies at 75–150 km depth beneath the Proterozoic terranes and at 30–220 km depth beneath the Archean terranes. In Phanerozoic regions, temperature variations alone can explain the observed velocities and gravity (van Greven et al., 2004).

Thermal lithosphere (defined here by a 1300 °C isotherm) along the profile is significantly thinner than seismic lithosphere (defined by a 2% velocity anomaly with respect to *ak135*) (Fig. 9b), in particular in

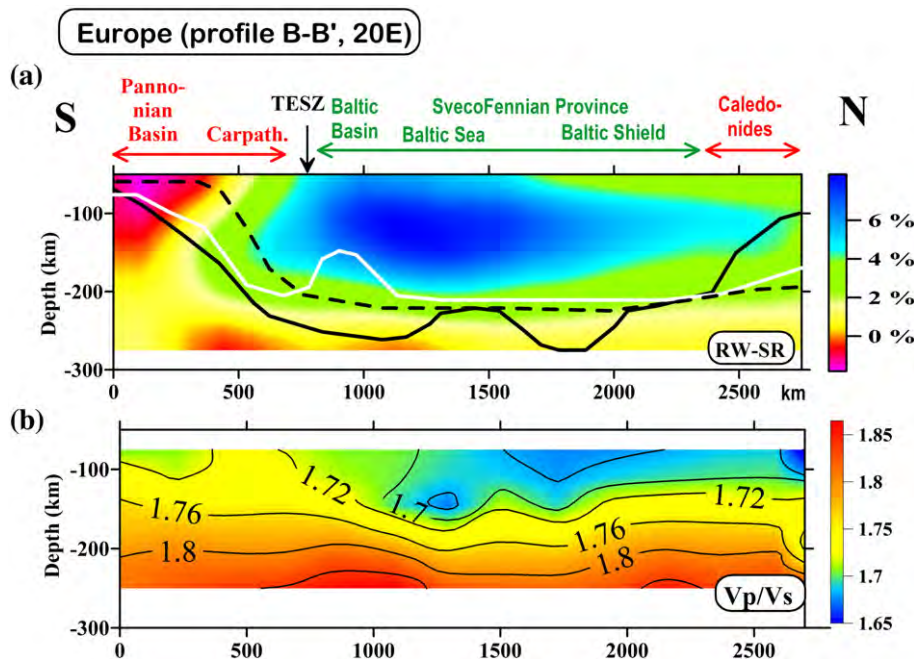


Fig. 10. Compositional (non-thermal) seismic velocity variations in the lithospheric mantle across Europe: (a) along 20E (profile B–B' in Fig. 8), (c) and (d) along 30E (profile C–C'). (b) and (e) V_p/V_s ratio along the profiles (after Artemieva, 2007). P-wave velocity is based on the regional model of Bijwaard and Spakman (2000); S-wave velocity is based on the model of Shapiro and Ritzwoller (2002). Seismic velocities (a), (c), (d) are based on the surface-wave tomography model of Shapiro and Ritzwoller, 2002 (a, d) and on the body-wave tomography model of Grand, 2002 (c). Black lines – lithospheric base as defined by a 2% ΔV_s anomaly with respect to *ak135* (Kennett et al., 1995) in the BW–G (solid lines) and RW–SR (dashed lines) tomography models; white lines – base of thermal lithosphere (defined by 1300 °C isotherm). Due to significantly different amplitudes of velocity anomalies in the BW–G and RW–SR seismic models, associated with different wave propagation in surface-wave and body-wave tomography, the results permit only a relative comparison of the compositional velocity anomalies, but not their absolute values (to facilitate the comparison, the color scales for two tomography models are shifted). Other notations as in Fig. 9. Abbreviations: OMB – Osninsk-Mikashkevichi Igneous Belt; SF – SvecoFennian Province. Diamonds – kimberlite locations in a 5-deg wide corridor along the profiles (Faure, 2006).

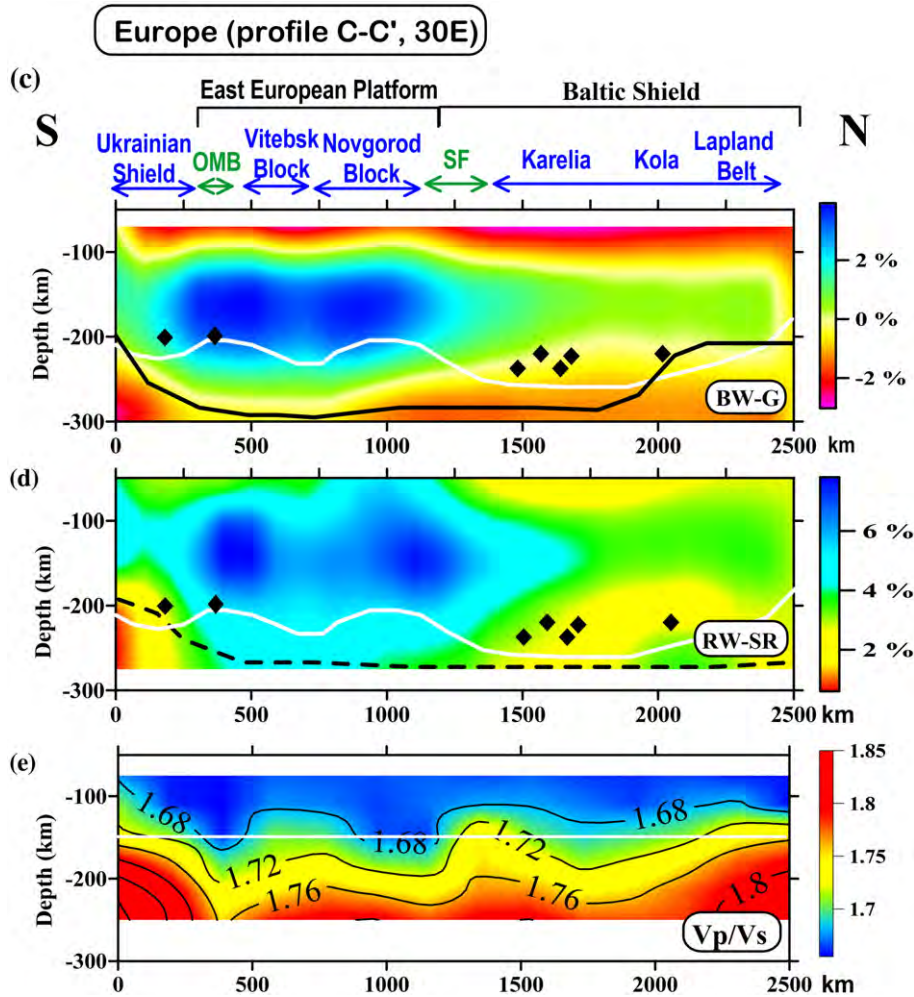


Fig. 10 (continued).

the central, Proterozoic part of the profile (note, however, an insufficient heat flow data coverage in the southern part of the Officer Basin (Fig. 8)). Theoretical analysis indicates that a discrepancy of up to 40–50 km may be expected between the base of seismic and thermal lithospheres in continental regions even with high seismic ray-path and borehole data coverage (Jaupart and Mareschal, 1999), chiefly because the sensitivity of seismic velocity variations to temperature variations decreases with depth, as the conductive geotherm approaches the mantle adiabat.

5.4.3. Europe

Fig. 10 shows two meridional cross-sections of the CLM of Europe. The profile along 20°E (B–B' in Fig. 8) starts in the Phanerozoic part of Europe, crosses the major tectonic boundary in Europe, the Trans-European Suture Zone (TESZ), which marks the western edge of the East European Craton, and continues further eastwards through the Paleoproterozoic terranes of the Baltic Shield. The TESZ is associated with a sharp change from low to high ΔV_s anomaly in the CLM, apparently caused by with the transition from fertile Phanerozoic to depleted cratonic lithospheric mantle. This conclusion is supported by gravity modeling which, similar to the cratonic edge in Australia, indicates a sharp density decrease of the CLM across the TESZ (Kaban et al., 2003).

Within the Paleoproterozoic CLM, a high velocity anomaly (with the strongest amplitude beneath the Baltic Sea) extends to a depth of ca. 200 km, where the amplitude of ΔV_s sharply decreases by at least 2% over a depth interval of <50 km. This abrupt change in non-thermal

part of seismic velocity anomaly apparently marks the base of the CBL and, within the resolution of the models, coincides with the bases of thermal and seismic lithospheres (Fig. 10a). The thickness of the CBL (“petrologic lithosphere”) reduces northwards; although the lithospheric mantle beneath the northern part of the Norwegian Caledonides (500–400 Ma) has positive ΔV_s , the amplitude of the anomaly is significantly weaker than beneath the SvecoFennian Province (2.0–1.8 Ga) of the Baltic Shield.

This result is consistent with the analysis of the V_p/V_s ratio (Artemieva, 2007) which is more sensitive to variation in composition than in temperature (Lee, 2003). Variations of the V_p/V_s ratio along the 20°E cross-section support the conclusion that petrologic lithosphere beneath the Proterozoic part of the Baltic Shield is ca. 150–175 km thick (Fig. 10b). Similarly, along the 30°E cross-section, the base of the petrologic lithosphere is at ca. 150–200 km beneath the Archean-Paleoproterozoic parts of the East European Platform and slightly shallows eastwards towards the Archean provinces of the Baltic Shield (Fig. 10e). Here I assume that the transition from the lithospheric mantle to the asthenosphere corresponds to $V_p/V_s \geq 1.72$, while calculations of synthetic V_p/V_s ratio for cratonic mantle xenoliths from the Kaapvaal lithospheric mantle indicate that the transition from low-T to high-T peridotites occurs at $V_p/V_s \geq 1.78$ (James et al., 2004). Note, however, that all synthetic V_p/V_s values are significantly higher than calculated for Europe from two tomography model (Fig. 10b,e) and fall between 1.75 and 1.78 at depths >100 km (James et al., 2004). At 250 km depth, values of the V_p/V_s ratio are uniform (ca. 1.80) along both of the profiles, probably due to the loss of resolution at this

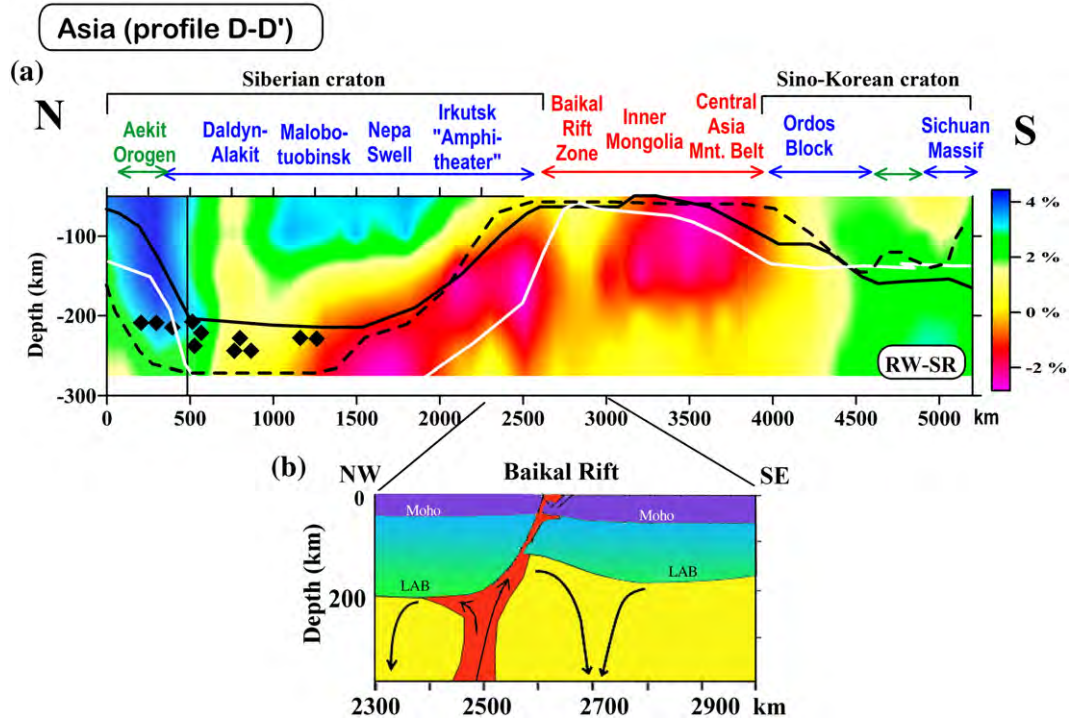


Fig. 11. (a) Compositional (non-thermal) seismic velocity variations in the lithospheric mantle across Asia (profile D-D' in Fig. 8). Seismic velocities are based on the surface-wave tomography model of Shapiro and Ritzwoller, 2002. Notations as in Fig. 9. Diamonds—kimberlite locations in a 5 deg-wide corridor along the profile (Faure, 2006). White shading at the left (the Aekit orogen): region where seismic and thermal estimates of the lithospheric thickness are significantly different (due to poor ray path coverage, uncertain crustal structure, and scarce borehole data, compare with Fig. 8), leading to an ambiguity in interpretation of compositional velocity anomalies. (b) Simplified geodynamic model for the Baikal Rift zone and the adjacent provinces (modified after Petit et al., 1998). The model suggests that the mantle anomaly is located beneath the Siberian craton and the rising hot material follows the bottom of the cratonic lithosphere and is guided underneath the Baikal Rift by the edge of the craton.

depth in the surface-wave model and fall within the range calculated for high-T lherzolite from the Kaapvaal (James et al., 2004).

Fig. 10c, d show the velocity cross-section along the 30°E meridian (C-C' in Fig. 8). The profile cuts the north-eastern blocks of the Archean-Paleoproterozoic Ukrainian Shield, the Osninsk-Mikashevichi Igneous Belt (a continental arc accreted to the western margin of the East

European Craton in Paleoproterozoic), the Vitebsk and Novgorod terranes (granulitic blocks, probably Archean in age, within the Paleoproterozoic terranes of the East European Craton), and continues into the Baltic Shield where it traverses the oldest terrane of the Baltic Shield, the Archean Karelian province (3.1–2.5 Ga), the northern part of the Archean-Neoproterozoic Kola Province, and the Paleoproterozoic

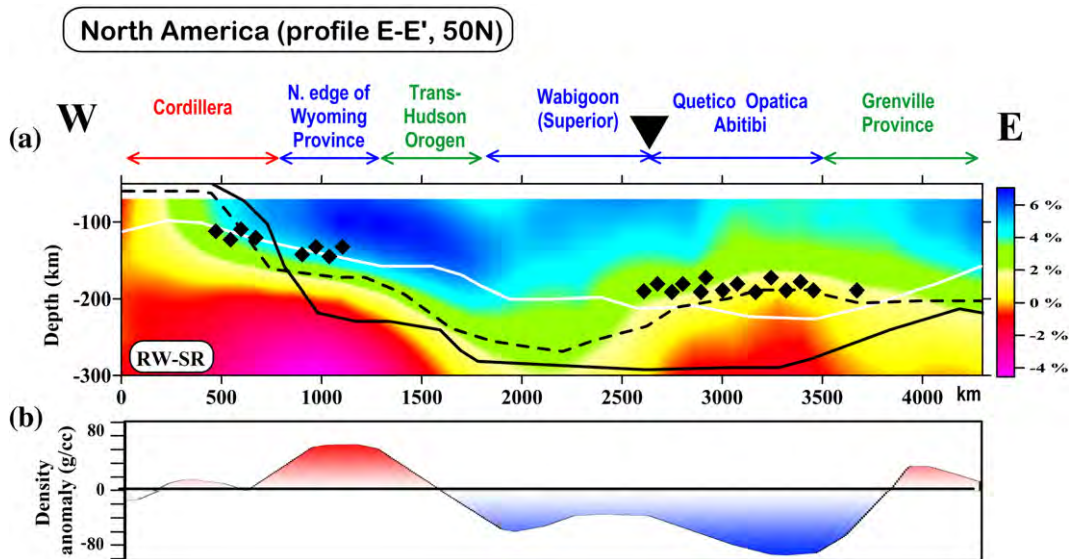


Fig. 12. (a) Compositional (non-thermal) seismic velocity variations in the lithospheric mantle across North America (profile E-E' in Fig. 8 along 50 N). Seismic velocities are based on the surface-wave tomography model of Shapiro and Ritzwoller, 2002. Notations as in Fig. 9. Diamonds—kimberlite locations in a 5 deg-wide corridor along the profile (Faure, 2006). Black triangle – the boundary between two lithospheric terranes as revealed by high-resolution seismic tomography and shear wave splitting study (Frederiksen et al., 2007). (b) Density anomaly of non-thermal origin in the lithospheric mantle along the same profile (after Kaban et al., 2003; Kaban et al., 2004, personal communication). The plot shows density effect integrated over the entire thickness of the lithospheric mantle so that the depth distribution of density anomaly is unknown.

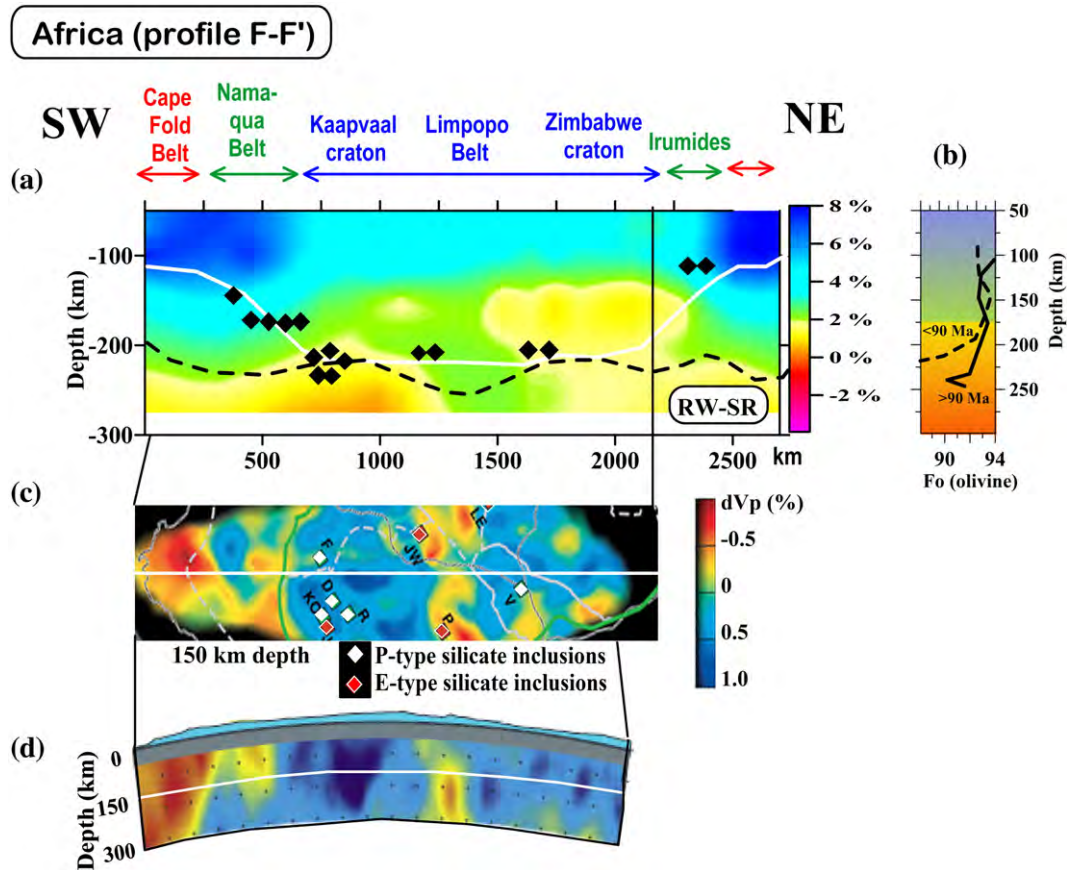


Fig. 13. Compositional (non-thermal) seismic velocity variations in the lithospheric mantle across South Africa (profile F–F' in Fig. 8). Seismic velocities are based on the surface-wave tomography model of Shapiro and Ritzwoller, 2002 (a). Notations as in Fig. 9. Diamonds–kimberlite locations in a 5 deg-wide corridor along the profile (Faure, 2006). (b) Depth distribution of Fo in Kaapvaal for mantle peridotites emplaced at >90 Ma and <90 Ma (modified after Gaul et al., 2000). Note that a depth of ca. 175 km where olivine content starts rapidly decreasing correlates with depth (within the model resolution) where seismic velocities decrease (a). (c) P-wave velocity variations at a 150 km depth approximately along the F–F' profile (modified from Shirey et al., 2003). (d) Velocity cross-section along the profile F–F' [it is profile B–B' of the Kaapvaal Project and its location is shown by white line in (c)] (modified from James et al., 2004). Note anticorrelation between the signs of seismic P-velocity variations and compositional S-velocity variations. Region with slow P-wave velocities and with E-type diamonds in the central part of the profile correlates with region of high non-thermal S-wave velocities.

Lapland Granulite Belt. The cross-section does not show any surprises in its southern part, within the East European Platform, where both the TBL and the CBL apparently extend down to 200–250 km, while seismic lithosphere extends slightly deeper, to ca. 250–300 km both in the BW–G and RW–SR seismic models. As mentioned earlier, significantly different amplitudes of velocity anomalies in the BW–G and RW–SR models (ca. 3% and 4–6%, correspondingly, Fig. 10c, d), associated with different wave propagation in surface-wave and body-wave tomography models and different inversion parameterizations, permit only a relative comparison of the compositional velocity anomalies, but not the absolute values (note different color scales for two tomography models).

The CLM in the northern part of the 30°E meridional cross-section (Fig. 10c, d) exhibits a significantly different pattern of compositional variations from that in its southern part. Contrary to expected, the lithospheric mantle of the Archean Central Karelia does not show high positive ΔV_s anomaly typical for depleted cratonic lithosphere; instead it has moderate to low ΔV_s and slightly higher V_p/V_s ratio at a depth of ca. 150 km (white line in Fig. 10e) which can be interpreted as northwards shallowing of CBL, while thickness of seismic and thermal lithosphere does not change along the profile (Fig. 10c, d). Furthermore, even the deepest xenoliths from the Karelian kimberlite pipes (from ca. 240 km depth) do not show any shearing (Kukkonen and Peltonen, 1999), which is commonly interpreted as an indicator of the base of the TBL.

Compositional (possibly lower-depletion) anomaly in the CLM in the northern part of the profile is clearly associated with the Archean terranes affected by kimberlite magmatism (emplaced at 589–626 Ma,

Lehtonen et al., 2004). The relative difference in the ΔV_s amplitudes between the CLM of the East European Platform (which, along the entire profile, remained tectonically undisturbed since the Paleoproterozoic) and the Karelian Province of the Baltic Shield (where kimberlite magmatism followed pre-existing lithosphere weakness zones) is ca. 2–3% for both body-wave and surface-wave tomography models used in this study (Fig. 10c, d). This velocity reduction in a “typical” cratonic CLM may be caused by metasomatic enrichment of the cratonic mantle by basaltic components during larger-scale pre-kimberlite magmatic events, which weakened the cratonic lithosphere and created conditions facilitating later kimberlite emplacement. The region affected by such a process could be significantly larger than the surface manifestation of kimberlite magmatism, for which a low-percentage mantle melting is typical.

These results indicate that past tectono-magmatic events (not necessarily limited to kimberlite-type magmatism, but marked at the surface by kimberlite emplacements) caused strong compositional alteration of the cratonic lithosphere. If so, the “typical” cratonic CLM in the core parts of the cratons, where no mantle-derived xenoliths are known, may have composition (and as a consequence, densities and seismic velocities) significantly different than those measured on xenolith samples.

Global gravity analysis (see Fig. 14 in Kaban et al., 2003) indicates that compositional density deficit in the lithospheric mantle of two Archean cratons, the Kola-Karelia province of the Baltic Shield and the Kalahari craton, is significantly lower than in other Archean cratons and, when compared with the global xenolith data, has density deficit

values more typical for Neoproterozoic regions. Noteworthy, the largest density deficit was calculated for the lithospheric mantle of Pilbara and Yilgarn cratons, where kimberlite magmatism is unknown (Kaban et al., 2003).

5.4.4. Asia

To examine if kimberlite magmatism is commonly associated with a depletion anomaly in the cratonic CLM, lateral and vertical regional variations of seismic velocity anomalies of non-thermal origin were calculated along the profile D–D' (see Fig. 8 for location). This profile passes the major kimberlite provinces of the Siberian craton (where kimberlites were emplaced both within the Proterozoic and the Archean terranes), the region of Cenozoic tectono-magmatic activity in the Baikal Rift Zone and in Inner Mongolia, and the terranes of the Archean–Paleoproterozoic Sino-Korean craton. For this cross-section two tomography models and the thermal model provide consistent estimates of the lithospheric thickness, which varies from 200–300 km beneath the Siberian craton to ca. 50 km in the Central Asia with an intermediate value of ca. 150 km for the Sino-Korean Craton, which has been significantly reworked in the Meso-Cenozoic (Menzies et al., 1993) (Fig. 11a).

The velocity anomalies of a non-thermal origin ΔV_s indicate a highly heterogeneous lithosphere structure along the profile. This conclusion agrees with xenolith data which indicate that, compositionally, the CLM of the Siberian craton is highly heterogeneous, with significant compositional variations observed from pipe to pipe, often over distances of a hundred km only (Gaul et al., 2000). Surprisingly, high values of ΔV_s are observed only at the north-eastern edge of the Siberian craton (Fig. 11a), within the Proterozoic Aekit Orogen, where several non-diamondiferous kimberlites were emplaced chiefly at 110–140 Ma. However, small lateral dimensions of this terrane are at the limit of the lateral resolution of the tomography model and, thus, could be a modeling artifact. The major diamondiferous kimberlite fields within the Siberian craton, emplaced at 344–367 Ma (see references in Faure, 2006) in the Daldyn-Alakit and Malo-Botuobinsk terranes, are associated with a very weak positive ΔV_s anomaly, similar to the Karelian province of the Baltic Shield (Fig. 10c,d). No CBL can be distinguished by ΔV_s beneath the Daldyn-Alakit terrane, where most of the Devonian kimberlites were erupted (Fig. 11a). Kimberlites of the Malo-Botuobinsk terrane were emplaced at the northern edge of the highly depleted cratonic nucleus, where the CBL (defined by a high positive ΔV_s anomaly) extends down to only a 120–150 km depth. Meanwhile, low seismic velocities indicative of the change in mantle rheology and marking the base of the seismic lithosphere are not observed down to at least a 200 km depth.

The transition from the Siberian craton to the Baikal Rift zone is marked by a sharp change in mantle properties. The depth where ΔV_s anomalies require presence of fluids or near-solidus temperatures changes from ca. 150–200 km beneath the Nera Swell and the so-called Irkutsk amphitheater (the flank zone of the Siberian craton along the north-eastern edge of the Baikal Rift Zone with the slightly elevated topography) to ca. 50 km beneath the regions of Cenozoic tectonic and magmatic activity in Central Asia. Surprisingly, the anomaly is not vertical in shape and extends far northwards (at least over several hundred kilometers) beneath the Siberian Craton. The anomaly beneath the regions of Cenozoic basaltic magmatism in Inner Mongolia is more localized both vertically and laterally.

Although the discussion of the origin of the Baikal Rift Zone is far beyond the scope of the present study, the results presented in Fig. 11a suggest that the major thermal anomaly in the mantle, probably associated with mantle melting, is located beneath the edge of the Siberian craton but not beneath the rift. Lower than “typical” degree of depletion of the cratonic mantle beneath the Malo-Botuobinsk terrane and the Nera Swell of the Siberian craton may be a direct manifestation of an interaction of uprising magmas with the lower part of the cratonic lithosphere. On its way upwards, the zone of

melting follows the cratonic edge, reaching the surface at the edge of the craton, at the Baikal Rift Zone (Fig. 11b). The pattern of observed ΔV_s variations can be best explained by the presence of thermal anomaly in the sublithospheric mantle beneath the Siberian craton (associated either with the presence of a plume or a convective instability in the mantle), which is effectively diverted by dry depleted lithospheric keel outwards of the craton interior. This conclusion is supported by recent studies of seismic anisotropy around the Baikal Rift which suggest the presence of horizontal asthenospheric flow perpendicular to the rift axis and directed from beneath the Siberian craton towards the thin Baikal–Mongolian lithosphere with no evidence for vertical flow beneath the axial zone of the Baikal Rift (Lebedev et al., 2006).

5.4.5. North America

The latitudinal profile of lateral and vertical variations of seismic velocity anomalies of non-thermal origin across North America (profile E–E' along 50°N, see Fig. 8 for location) further supports the conclusion that kimberlites are associated with regions with a significant compositional modification of the cratonic lithospheric mantle, i.e. with a general increase in its fertility accompanied by a general decrease in seismic velocities (Fig. 12a). The profile has been chosen to follow the northern edge of the area within the Canadian Shield with a good coverage by heat flow measurements.

Similarly to the cross-sections across Europe and Australia, the transition from Phanerozoic to cratonic lithosphere is marked by a sharp change in ΔV_s . In agreement with xenolith data, thermal and seismic tomography models indicate that at the northernmost edge of the Archean Wyoming craton the lithosphere was eroded to ca. 150 km thickness. Lithospheric mantle of the Wyoming craton is dense (Fig. 12b) and fertile. Since the lateral dimension of the Wyoming craton along the profile is less than 500 km, strong positive ΔV_s anomaly in its lithospheric mantle is, apparently, smeared from the strong positive anomaly in the CLM of the western Canadian Shield. Positive ΔV_s anomaly in the lithospheric mantle continues further east where it can be associated with the Archean terrane buried within the Paleoproterozoic Trans-Hudson Orogen (the Sask craton) (Ashton et al., 1999).

Similar to the pattern observed for the kimberlite provinces of the Baltic Shield and Siberia, the compositional anomaly reduces in amplitude in the region east of 85–90 °W, where kimberlite magmas were emplaced in late Jurassic (Heaman and Kjarsgaard, 2000). These results are in a striking agreement with the recent high-resolution seismic tomography and shear wave splitting study, which shows two distinct lithospheric domains in the Canadian Shield with the boundary at approximately 86–87°W at 50°N latitude (the Wabigoon–Wawa/Quetico boundary, Fig. 12) (Frederiksen et al., 2007). To the west of this boundary, the lithospheric mantle has strong anisotropy and high velocities, while to the east the average split times are twice less and average velocity anomaly reduces by 2.5% (relative to *iasp91*). In accord with the conclusions of these authors, the results of the present study indicate strong lateral compositional heterogeneity of the lithospheric mantle of the Superior Province. Lower than “typical” cratonic values of ΔV_s in the eastern part of the profile can reflect compositional modification of the cratonic lithosphere by a passage of the Great Meteor hotspot, followed by kimberlite magmatism. Note that, similar to the western part of the Superior Province, the Grenville Province which is underlain by the Archean lithospheric mantle has high values of ΔV_s , however it is not associated with a negative density anomaly as one might expect for depleted cratonic mantle (Fig. 12b).

5.4.6. South Africa

The profile across the best studied kimberlite province of the world confirms the conclusion that cratonic lithospheric mantle sampled by mantle-derived xenoliths may be non-representative of the “intact”

cratonic mantle (Fig. 13a). The profile starts at the Paleozoic Cape Fold Belt, crosses the Kalahari craton, and stops at the East African Rift where meaningful comparison of thermal and seismic models is precluded by the smearing effect of rifting-related mantle anomaly on seismic velocities in adjacent tectonic provinces (note a significant discrepancy between the base of thermal and seismic lithospheres at both ends of the profile).

Within the Kalahari craton, thickness of thermal lithosphere calculated from heat flow data (Ballard and Pollack, 1987; Jones, 1988; Artemieva and Mooney, 2001) agrees with xenolith constraints: xenolith geotherm intersects mantle adiabat at ca. 200–220 km depth (Rudnick and Nyblade, 1999). Similarly, geotherms calculated from regional seismic velocity profiles for mantle mineralogy beneath the Kaapvaal as indicated by mantle nodules brought to the surface estimate thermal lithosphere to be ca. 200 km thick (Kuskov et al., 2006; Priestley et al., 2006). Shearing in high-T peridotites indicate that the base of the rheologically strong lithospheric mantle in the Kaapvaal craton is at ca. 170–200 km (depending on combinations of thermobarometers) (e.g. Boyd, 1987).

In accord with thermal approaches, thickness of seismic lithosphere estimated from regional tomography models is ca. 200–250 km (Zhao et al., 1999; Ritsema and van Heijst, 2000; James et al., 2001; Freybourger et al., 2001) with slightly larger values of lithosphere thickness (250–300 km) estimated from global teleseismic tomography (e.g. Zhang and Tanimoto, 1993). Most of regional seismic studies indicate significant lateral and vertical seismic velocity variations in lithospheric mantle of the Kalahari craton. A relatively short-wavelength of many of these velocity variations (see e.g. Fig. 13c,d) precludes their interpretation in terms of regional temperature variations, since in the real Earth such temperature anomalies in the lithospheric mantle will be smeared by horizontal heat transfer. Consequently, it questions the validity of seismic velocity-to-temperature conversions unless short-wavelength variations in mantle mineralogy are incorporated into the calculations. In particular, sensitivity analysis for a conversion of seismic velocities to temperatures for mantle mineralogies typical of the Kaapvaal craton indicates that small differences between xenolith compositions lead to significant variations in inferred mantle temperatures (Kuskov et al., 2006).

An experimental study of oxygen fugacity provides support for a strong vertical compositional stratification of the lithospheric mantle beneath the Kaapvaal craton (Woodland and Koch, 2003): in the depth range between 80 and 150 km depth there is a progressive decrease of fugacity by 3 log units. At greater depth (150–220 km), a decrease in fugacity becomes weaker, only about 0.8 log units. Note that the depth gradient of fugacity changes at ca. 150 km depth. An increase in fugacity in Kimberly mantle at 140–160 km depth was interpreted as an indicator of a complex metasomatic history (Woodland and Koch, 2003).

The results of the present study indicate that the amplitude of composition-induced seismic variations in the lithospheric mantle sharply decreases at ca. 150 ± 25 km depth beneath the Kalahari craton and at a slightly deeper depth (200–250 km) beneath the Limpopo Belt (Fig. 13a). The decreasing amplitude of composition-induced anomaly may be interpreted as an indicator of the base of the chemical boundary layer. Based on receiver-function images of the depth to the transition zone beneath the Kaapvaal craton, thickness of the chemical boundary layer (petrologic lithosphere) was estimated to be between 160 and 370 km (Niu et al., 2004). Similarly, a significant chemical stratification of lithospheric mantle with a pronounced change at ca. 150 km depth has been reported in xenolith studies from the Kaapvaal (Fig. 13b), Slave and Siberian cratons (Griffin et al., 1999a,b; Gaul et al., 2000; Kopylova and Russell, 2000). For young peridotites from the Kaapvaal craton (<90 Ma, Fig. 13b), the decrease in forsterite content below ca. 175–200 km depth is significantly stronger than for the older population suggesting metasomatic modification of the lithospheric mantle by >90 Ma magmatism.

Region where non-thermal seismic velocity anomaly decreases starts at ca. 150 km depth beneath most of the Kalahari craton. At this depth, mantle temperature is ca. 1000–1100 °C (Artemieva and Mooney, 2001) and thus it is unlikely that velocity reduction can be explained by grain boundary relaxation at high temperatures as proposed by Priestley et al. (2006). A compositional origin of the anomaly is more likely. Unfortunately, data on mantle mineralogy provided by mantle nodules brought to the surface cannot shed light on the origin of the velocity anomaly since globally regions with high non-thermal velocity anomalies are not sampled by mantle-derived xenoliths (Figs. 9–13).

Some clue on the compositional origin of the anomaly can be got from a recent study by Shirey et al. (2003) who compared the results of regional P-wave tomography with composition and ages of diamonds. They found that regions with slow P-wave velocity in the lithospheric mantle in the northern Kaapvaal craton–Limpopo Belt correlate with a greater proportion of eclogitic rather than peridotitic silicate inclusions (Fig. 13c). The results of the present study show a striking anticorrelation between the signs of compositional S-velocity anomalies and seismic P-velocity anomalies (Fig. 13a,c,d): composition-induced S-velocities are slightly higher in the same region in the central part of the profile where slow P-wave velocity anomaly was observed by Shirey et al. (2003). An inversion of seismic velocity profiles beneath the Kaapvaal for two end-member mantle compositions (primitive mantle, PM, and garnet peridotite, GP) indicates that a shift in mantle composition towards PM or GP has opposite effects on P- and S-velocities: for GP mantle composition P-velocities are slightly less and S-velocities are slightly greater as compared to PM (Kuskov et al., 2006). Thus, the anomaly in the lithospheric mantle of the northern Kaapvaal craton–Limpopo Belt may be associated with its more depleted composition as compared to the Kaapvaal and Zimbabwe cratons. Alternatively, combining present results with the analysis of diamond inclusions (Shirey et al., 2003), one may argue that low velocities in the lithospheric mantle of the Kaapvaal and the Zimbabwe cratons, where P-type diamond inclusions are typical, may be associated with a higher diopside content (Harris and Gurney, 1979) (Table 2). A full interpretation of the results in terms of chemical anomalies is beyond the scope of this paper.

6. Conclusions

This study discusses different approaches to studies of the continental lithosphere. Based on joint analysis of global seismic tomography and thermal data, the following conclusions can be made.

1. Global V_s seismic tomography models (Grand, 2002; Shapiro and Ritzwoller, 2002) and a global thermal model (Artemieva and Mooney, 2001) provide consistent estimates of the lithospheric thickness beneath the continents. They outline the same regions of thick and thin lithosphere (Fig. 5), which are correlated with surface tectonics and with tectono-thermal ages (Artemieva, 2006) (Fig. 3).
2. Velocity anomalies of non-thermal origin ΔV_s (calculated from a joint analysis of seismic and thermal data) contribute significantly to seismic velocity anomalies. They show a strong correlation with surface tectonics and lithospheric ages (Fig. 7) and can be explained either by compositional heterogeneity of lithospheric mantle (associated primarily with iron-depletion of the cratonic lithosphere) or by presence of melts and fluids in the lithosphere of active regions.
3. In tectonically active regions, strong negative non-thermal (i.e. not caused by temperature variations alone) anomalies suggest presence of melts in the upper mantle. In particular, in the Baikal province of Siberia, the center of the melting anomaly is located in the upper mantle beneath the Siberian Platform rather than beneath the rift zone. The rim of the cratonic lithosphere guides the melting anomaly

on its way upwards, so that it reaches the surface at the Baikal Rift Zone at the edge of the Siberian craton (Fig. 11).

4. In cratons, the lateral size of the regions with positive compositional velocity anomalies diminishes with depth (Fig. 7), reflecting either a gradual lateral accretion of Proterozoic terranes to the Archean nuclei with significant variations in composition of the CLM, or a gradual inwards metasomatism, which is more dramatic in the deeper parts of the lithosphere.
5. In the cratonic regions, within the model resolution, the base of seismic lithosphere (defined by a 2% δV_s relative to $ak135$) commonly correlates with the base of thermal lithosphere and with the base of the chemical boundary layer (CBL) defined by a high gradient in ΔV_s (Figs. 9–13). However, in kimberlite provinces the base of the CBL does not correlate neither with seismic nor with thermal LAB, and the lithospheric mantle shows only weakly positive values of ΔV_s (Figs. 10–13). This pattern is interpreted as reflecting magmatism-related metasomatic enrichment of the cratonic lithosphere either prior or during kimberlite emplacement. The lateral dimensions of the areas with a reduced depletion are significantly larger than kimberlite provinces and can exceed 1000 km in diameter, suggesting, that kimberlite magmatism followed lithosphere weakness zones produced by earlier larger-tectono-magmatic events.
6. The results suggest that lithospheric mantle sampled by xenoliths brought to the surface by magmas may be non-representative of the intact cratonic mantle, implying that xenolith-based constraints on the composition of the CLM can be biased.

A further study based on high-resolution seismic data for a region with well constrained lithospheric temperatures and abundant xenolith data is needed to quantify the effects of magmatism on compositional modification of the cratonic lithosphere. Incorporation of gravity data into the analysis will further increase the reliability of the model constraints.

Acknowledgements

The author is grateful to Nikolai Shapiro, Mike Ritzwoller, and Steve Grand for a possibility to use their mantle seismic tomography models. Discussions with D. Eaton, M. Ritzwoller, M. Cara, E. Debayle, S.-I. Karato, M. Coltorti, S. Grand, and B. Romanowicz on various issues related to the study provided further insights into the topic. Reviews by Michel Gregoire and Claire Perry are gratefully acknowledged. Special thanks are to Nick Arndt for his detailed comments on the manuscript. Review sections of this paper contain material that was previously included into the Dr. Sci. (habil.) dissertation of I.M. Artemieva "Continental lithosphere: structure and evolution" (University of Copenhagen, 2007). The study is supported by a personal research grant of Carlsbergfondet, Denmark.

References

- Anderson, D.L., 1995. Lithosphere, asthenosphere, and perisphere. *Reviews of Geophysics* 33, 125–149.
- Anderson, O.L., Isaak, D.G., 1995. Elastic constants of mantle minerals at high temperature. In: a handbook of physical constants. American Geophysical Union Reference Shelf 2, 64–97.
- Anderson, O.L., Schreiber, E., Lieberman, R.C., Soga, M., 1965. Some elastic constant data on minerals relevant to geophysics. *Reviews of Geophysics* 6, 491–524.
- Artemieva, I.M., 2006. Global $1^\circ \times 1^\circ$ thermal model TC1 for the continental lithosphere: implications for lithosphere secular evolution. *Tectonophysics* 416, 245–277.
- Artemieva, I.M., 2007. Dynamic topography of the East European Craton: shedding light upon the lithospheric structure, composition and mantle dynamics. *Global and Planetary Change* 58, 411–434. doi:10.1016/j.gloplacha.2007.02.013.
- Artemieva, I.M., Mooney, W.D., 2001. Thermal structure and evolution of Precambrian lithosphere: a global study. *Journal of Geophysical Research* 106, 16387–16414.
- Artemieva, I.M., Mooney, W.D., 2002. On the relation between cratonic lithosphere thickness, plate motions, and basal drag. *Tectonophysics* 358, 211–231.
- Artemieva, I.M., Billien, M., L  v  que, J.-J., Mooney, W.D., 2004. Shear-wave velocity, seismic attenuation, and thermal structure of the continental upper mantle. *Geophysical Journal International* 157, 607–628.
- Artemieva, I.M., Thybo, H., Kaban, M.K., 2006. Deep Europe today: geophysical synthesis of the upper mantle structure and lithospheric processes over 3.5 Ga. *Geological Society, London, Memoirs* 32, 11–41.
- Ashton, K.E., Heaman, L.M., Lewry, J.F., Hartlaub, R.P., Shi, R., 1999. Age and origin of the Jan Lake Complex: a glimpse at the buried Archean craton of the Trans-Hudson Orogen. *Canadian Journal of Earth Sciences* 36 (2), 185–208. doi:10.1139/cjes-36-2-185.
- Ballard, S., Pollack, H.N., 1987. Diversion of heat by Archean cratons: a model for southern Africa. *Earth and Planetary Science Letters* 85, 253–264.
- Barrel, J., 1914. The strength of the Earth's crust. *Journal of Geology* 22, 87.
- Bassin, C., Laske, G., Masters, G., 2000. The current limits of resolution for surface wave tomography in North America. *Eos, Transactions of American Geophysical Union* 81, F897.
- Bechtel, T.D., Forsyth, D.W., Sharpston, V.L., Grieve, R.A.F., 1990. Variations in effective elastic thickness of the North American lithosphere. *Nature* 343, 636–638.
- Benfield, A.E., 1939. Terrestrial heat flow in Britain. *Proceedings of the Royal Society* 173, 428–450.
- Ben Ismail, W., Mainprice, D., 1998. An olivine fabric database: an overview of upper mantle fabrics and seismic anisotropy. *Tectonophysics* 296, 145–157.
- Bijwaard, H., Spakman, W., 2000. Non-linear global P-wave tomography by iterated linearized inversion. *Geophysical Journal International* 141, 71–82.
- Birch, F., Roy, E.R., Decker, E.R., 1968. Heat flow and thermal history and New England and New York. In: An-Zen, E. (Ed.), *Studies of Appalachian geology*. Wiley, Interscience, New York, pp. 437–451.
- Bodine, J.H., Steckler, M.S., Watts, A.B., 1981. Observations of flexure and the rheology of the oceanic lithosphere. *Journal of Geophysical Research* 86, 3695–3707.
- Boyd, F.R., 1973. A pyroxene geotherm. *Geochimica and Cosmochimica Acta* 37, 2533–2546.
- Boyd, F.R., 1987. High- and low-temperature garnet peridotite xenoliths and their possible relation to the lithosphere–asthenosphere boundary beneath southern Africa. In: Nixon, P.H. (Ed.), *Mantle xenoliths*. Wiley, Chichester, pp. 403–412.
- Boyd, F.R., 1989. Compositional distinction between oceanic and cratonic lithosphere. *Earth and Planetary Science Letters* 96, 15–26.
- Boyd, F.R., McCallister, R.H., 1976. Densities of fertile and sterile garnet peridotites. *Geophysical Research Letters* 3, 509–512.
- Boyd, F.R., Pearson, D.G., Mertzman, S.A., 1999. Spinnet-facies peridotites from the Kaapvaal root. In: Gurney, J.J., Gurney, J.L., Pascoe, M.D., Richardson, S.H. (Eds.), *Proceedings of 7th International Kimberlite Conference*, vol. 1, pp. 40–48.
- Brey, G.P., Kogarko, L.N., Ryabchikov, I.D., 1991. Neues Jahrbuch fuer Mineralogie. *Monatshefte* 4, 159–168.
- Bullard, E.C., 1939. Heat flow in South Africa. *Proceedings of the Royal Society* 173, 474–502.
- Cm  ral, M., Fitz Gerald, J.D., Faul, U.F., Green, D.H., 1998. A close look at dihedral angles and melt geometry in olivine–basalt aggregates: a TEM study. *Contributions to Mineralogy and Petrology* 130, 336–345. doi:10.1007/s004100050369.
- Constable, S., Shankland, T.J., Duba, A., 1992. The electrical conductivity of an isotropic olivine mantle. *Journal of Geophysical Research* 97, 3397–3404.
- De Rito, R., Gozzarelli, F., Hodge, D., 1986. A forward approach to the problem of nonlinear viscoelasticity and the thickness of the mechanical lithosphere. *Journal of Geophysical Research* 91, 8295–8313.
- Deschamps, F., Trampert, J., Snieder, R., 2002. Anomalies of temperature and iron in the uppermost mantle inferred from gravity data and tomographic models. *Physics of Earth and Planetary Interior* 129, 245–264.
- Djomani, P.Y.H., O'Reilly, S.Y., Griffin, W.L., Morgan, P., 2001. The density structure of subcontinental lithosphere through time. *Earth and Planetary Science Letters* 184, 605–621.
- Duffy, T.S., Anderson, D.L., 1989. Seismic velocities in mantle minerals and the mineralogy of the upper mantle. *Journal of Geophysical Research* 94, 1895–1912.
- Everett, J.D., 1883. Report for British Association for 1882, pp. 72–90.
- Fan, W.M., Zhang, H.F., Baker, J., 2000. On and off the North China Craton: where is the Archean keel? *Journal of Petrology* 41, 933–950.
- Faul, U.H., 1997. Permeability of partially molten upper mantle rocks from experiments and percolation theory. *Journal of Geophysical Research* 102, 10299–10311.
- Faul, U.H., Jackson, I., 2005. The seismological signature of temperature and grain size variations in the upper mantle. *Earth and Planetary Science Letters* 234, 119–134.
- Faure S., 2006. World Kimberlites and Lamproites CONSOREM Database (Version 2006-1). Consortium de Recherche en Exploration Min  rale CONSOREM, Universit   du Qu  bec    Montr  al, www.consorem.ca.
- Finnerty, A.A., Boyd, F.R., 1987. Thermobarometry for garnet peridotites: basis for the determination of thermal and compositional structure of the upper mantle. In: Nixon, P.H. (Ed.), *Mantle Xenoliths*. Wiley and Sons, pp. 381–402.
- Fort  , A.M., Perry, H.K.C., 2000. Geodynamic evidence for a chemically depleted continental tectonosphere. *Science* 290, 1940–1944.
- Fort  , A.M., Woodward, R.L., Dziewonski, A.M., 1994. Joint inversions of seismic and geodynamic data for models of three-dimensional mantle heterogeneity. *Journal of Geophysical Research* 99, 21857–21887.
- Frederiksen, A.W., Miong, S.-K., Darbyshire, F.A., Eaton, D.W., Rondenay, S., Sol, S., 2007. Lithospheric variations across the Superior Province, Ontario, Canada: Evidence from tomography and shear wave splitting. *Journal of Geophysical Research* 112, B07318. doi:10.1029/2006JB004861.
- Freyburger, M., Gaherty, J.B., Jordan, T.H., Kaapvaal Seismic Group, 2001. Structure of the Kaapvaal craton from surface waves. *Geophysical Research Letters* 28, 2489–2492.
- Furlong, F.P., Spakman, W., Wortel, R., 1995. Thermal structure of the continental lithosphere: constraints from seismic tomography. *Tectonophysics* 244, 107–117.
- Gaul, O.F., Griffin, W.L., O'Reilly, S.Y., Pearson, N.J., 2000. Mapping olivine composition in the lithospheric mantle. *Earth and Planetary Science Letters* 182, 223–235.

- Garfunkel, Z., 2007. Controls of stable continental lithospheric thickness: the role of basal drag. *Lithos* 96, 299–314.
- Godey, S., Deschamps, F., Trampert, J., Snieder, R., 2004. Thermal and compositional anomalies beneath the North American continent. *Journal of Geophysical Research* 109, B01308. doi:10.1029/2002JB002263.
- Goes, S., van der Lee, S., 2002. Thermal structure of the North American uppermost mantle inferred from seismic tomography. *Journal of Geophysical Research*, 107, 5276–5289.
- Goes, S., Govers, R., Vacher, P., 2000. Shallow upper mantle temperatures under Europe from P and S wave tomography. *Journal of Geophysical Research* 105, 11153–11169.
- Goes, S., Simons, F.J., Yoshizawa, K., 2005. Seismic constraints on temperature of the Australian uppermost mantle. *Earth and Planetary Science Letters* 236, 227–237.
- Grand, S.P., 2002. Mantle shear-wave tomography and the fate of subducted slabs. *Philosophical Transactions of the Royal Society of London. Series A*, 360, 2475–2491.
- Gribb, T.T., Cooper, R.F., 1998. Low-frequency shear attenuation in polycrystalline olivine: grain boundary diffusion and the physical significance of the Andrade model for viscoelastic rheology. *Journal of Geophysical Research* 103, 27267–27279.
- Griffin, W.L., Ryan, C.G., 1995. Trace elements in indicator minerals: area selection and target evaluation in diamond exploration. *Journal of Geochemical Exploration* 53, 311–337.
- Griffin, W.L., O'Reilly, S.Y., Ryan, C.G., Gaul, O., Ionov, D., 1998. Secular variation in the composition of continental lithospheric mantle. In: Braun, J. (Ed.), *Structure and evolution of the Australian continent*. American Geophysical Union Geodynamics Series, vol. 26, pp. 1–25.
- Griffin, W.L., Ryan, C.G., Kaminsky, F.V., O'Reilly, S.Y., Natapov, L.M., Win, T.T., Kinny, P.D., Ilupin, I.P., 1999a. The Siberian lithosphere traverse: mantle terranes and the assembly of the Siberian Craton. *Tectonophysics* 310, 1–35.
- Griffin, W.L., O'Reilly, S.Y., Ryan, C.G., 1999b. The composition and origin of continental lithospheric mantle. In: Fei, Y., Bertka, C.M., Mysen, B.O. (Eds.), *Mantle petrology: Field observations and high pressure experimentation: A tribute to Francis R. (Joe) Boyd*. Geochemical Society Special Publication, vol. 6, pp. 13–45.
- Grutter, H.S., Moore, R.O., 2003. Pyroxene geotherms revisited – an empirical approach based on Canadian xenoliths. *Proceedings of 8th International Kimberlite Conference*, Victoria, BC, Canada. FLA-0272.
- Gutenberg, B., 1954. Low-velocity layers in the Earth's mantle. *Geological Society of America Bulletin* 65, 337–347.
- Harris, J.W., Gurney, J.J., 1979. Inclusions in diamond. In: Field, J.E. (Ed.), *The Properties of Diamond*. Academic Press, New York, pp. 555–591.
- Hawkesworth, C.J., Kempton, P.D., Rogers, N.W., Ellam, R.M., van Calsteren, P.W., 1990. Continental mantle lithosphere, and shallow level enrichment process in the Earth's mantle. *Earth and Planetary Science Letters* 96, 256–268.
- Heaman, L.M., Kjarsgaard, B.A., 2000. Timing of eastern North American kimberlite magmatism: Continental extension of the Great Meteor hotspot track? *Earth and Planetary Science Letters* 178, 253–268.
- Hirth, G., Evans, R.L., Chave, A.D., 2000. Comparison of continental and oceanic mantle electrical conductivity: is the Archean lithosphere dry? *Geochemistry, Geophysics and Geosystems* 1 doi:10.1029/2000GC000048.
- Ito, K., Kennedy, G.C., 1967. Melting and phase relations in a natural peridotite to 40 kilobars. *American Journal of Sciences* 265, 519–538.
- Jackson, I., 2000. Laboratory measurement of seismic wave dispersion and attenuation: recent progress. *Geophysical Monograph* 117, 265–289.
- Jackson, I., Rudnick, R.L., O'Reilly, S.Y., Bezant, C., 1990. Measured and calculated elastic wave velocities for xenoliths from the lower crust and upper mantle. *Tectonophysics* 173, 207–210.
- Jackson, I., Paterson, M.S., Fitz Gerald, J.D., 1992. Seismic wave dispersion and attenuation in heim dunite: an experimental study. *Geophysical Journal International* 108, 517–534.
- Jaeger, J.C., 1965. Application of the theory of heat conduction to geothermal measurements. *American Geophysical Union Monograph*, vol. 8.
- James, D.E., Boyd, F.R., Schutt, D., Bell, D.R., Carlson, R.W., 2004. Xenolith constraints on seismic velocities in the upper mantle beneath South Africa. *Geochemistry, Geophysics and Geosystems* 5 (1), Q01002. doi:10.1029/2003GC000551.
- James, D.E., Fouch, M.J., VanDecar, J.C., van der Lee, S., Kaapvaal Seismic Group, 2001. Tectospheric structure beneath southern Africa. *Geophysical Research Letters* 28, 2485–2488.
- Jaupart, C., Mareschal, J.-C., 1999. Thermal structure and thickness of continental roots. *Lithos* 48, 93–114.
- Jones, M.Q.W., 1988. Heat flow in the Witwatersrand Basin and environs and its significance for the South African Shield geotherm and lithosphere thickness. *Journal of Geophysical Research* 93, 3243–3260.
- Jordan, T.H., 1975. The continental tectosphere. *Reviews of Geophysics and Space Physics* 13 (3), 1–12.
- Jordan, T.H., 1978. Composition and development of the continental tectosphere. *Nature* 274, 544–548.
- Jordan, T.H., 1979. Mineralogies, densities and seismic velocities of garnet lherzolites and their geophysical implications. In: Boyd, F.R., Meyer, H.O.A. (Eds.), *The mantle sample: Inclusions in kimberlite and other volcanics*. American Geophysical Union, Washington, D.C., pp. 1–14.
- Jordan, T.H., 1988. Structure and formation of the continental tectosphere. *Journal of Petrology* 29, 11–37.
- Jordan, T.H., 1997. Petrologic controls on the density and seismic velocities of the cratonic upper mantle. *Eos, Transactions of the American Geophysical Union* 78 (46), F746.
- Kaban, M.K., Schwintzer, P., Artemieva, I.M., Mooney, W.D., 2003. Density of continental roots: compositional and thermal effects. *Earth and Planetary Science Letters* 209, 53–69.
- Kaban, M.K., Schwintzer, P., Reigber, C., 2004. A new isostatic model of the lithosphere and gravity field. *Journal of Geodesy* 78, 368–385.
- Kampfmann, W., Berckhemer, H., 1985. High temperature experiments on the elastic and anelastic behavior of magmatic rocks. *Physics of Earth and Planetary Interior* 40, 223–247.
- Karato, S.-I., 1993. Importance of anelasticity in the interpretation of seismic tomography. *Geophysical Research Letters* 20, 1623–1626.
- Karato, S., Spetzler, H.A., 1990. Defect microdynamics in minerals and solid state mechanisms of seismic wave attenuation and velocity dispersion in the mantle. *Reviews of Geophysics* 28 (4), 399–421.
- Karato, S., Wu, P., 1993. Rheology of the upper mantle: a synthesis. *Science* 260, 771–777.
- Katsura, T., Yamada, H., Nishikawa, O., 2004. Olivine-wadsleyite transition in the system (Mg,Fe)₂SiO₄. *Journal of Geophysical Research* 109, Article Number: B02209.
- Kennett, B.L.N., 2006. On seismological reference models and the perceived nature of heterogeneity. *Physics of the Earth and Planetary Interior* 159, 129–139.
- Kennett, B.L.N., Engdahl, E.R., 1991. Travel times for global earthquake location and phase identification. *Geophysical Journal International* 105, 429–465.
- Kennett, B.L.N., Engdahl, E.R., Buland, R., 1995. Constraints on seismic velocities in the Earth from traveltimes. *Geophysical Journal International* 122, 108–124.
- Kopylova, M.G., Russell, J.K., 2000. Chemical stratification of cratonic lithosphere: constraints from the Northern Slave craton, Canada. *Earth and Planetary Science Letters* 181, 71–87.
- Krige, L.J., 1939. Borehole temperatures in Transvaal and Orange Free State. *Proceedings of the Royal Society* 173, 450–474.
- Kukkonen, I.T., Peltonen, P., 1999. Xenolith-controlled geotherm for the central Fennoscandian Shield: implications for lithosphere–asthenosphere relations. *Tectonophysics* 304, 301–315.
- Kushiro, I., Syono, Y., Akimoto, S., 1968. Melting of a peridotite nodule at high pressures and high water pressures. *Journal of Geophysical Research* 73, 6023–6029.
- Kuskov, O.L., Kronrod, V.A., Annersten, H., 2006. Inferring upper-mantle temperatures from seismic and geochemical constraints: implications for Kaapvaal craton. *Earth and Planetary Science Letters* 244, 133–154.
- Kuznir, N., Karner, G., 1985. Dependence of the flexural rigidity of the continental lithosphere on rheology and temperature. *Nature* 316, 138–142.
- Lachenbruch, A.H., 1970. Crustal temperature and heat production: implications of the linear heat-flow relation. *Journal of Geophysical Research* 75, 3291–3300.
- Lebedev, S., Meier, T., van der Hilst, R.D., 2006. Asthenospheric flow and origin of volcanism in the Baikal Rift area. *Earth and Planetary Science Letters* 249, 415–424.
- Ledo, J., Jones, A.G., 2005. Upper mantle temperature determined from combining mineral composition, electrical conductivity laboratory studies and magnetotelluric field observations: application to the intermontane belt, Northern Canadian Cordillera. *Earth and Planetary Science Letters* 236, 258–268.
- Lee, C.-T.A., 2003. Compositional variation of density and seismic velocities in natural peridotites at STP conditions: implications for seismic imaging of compositional heterogeneities in the upper mantle. *Journal of Geophysical Research* 108, 2441. doi:10.1029/2003JB002413.
- Lee, C.T., Rudnick, R.L., 1999. Compositionally stratified cratonic lithosphere: petrology and geochemistry of peridotite xenoliths. In: Gurney, J.J., Gurney, J.L., Pascoe, M.D., Richardson, S.H. (Eds.), *Proceedings of 7th International Kimberlite Conference*, vol. 2, pp. 503–521.
- Lehmann, I., 1961. S and the structure of the upper mantle. *Geophysical Journal of the Royal Astronomical Society* 4, 124–138.
- Lehmann, I., 1962. The travel times of the longitudinal waves of the Logan and Blanca atomic explosions and their velocities in the upper mantle. *Bulletin of the Seismological Society of America* 52, 519–526.
- Lehtonen, M.L., O'Brien, H.E., Peltonen, P., Johanson, B.S., Pakkanen, L.K., 2004. Layered mantle at the Karelian Craton margin: P-T of mantle xenocrysts and xenoliths from the Kaavi-Kuopio kimberlites, Finland. *Lithos* 77, 593–608.
- Lenardic, A., Moresi, L., 2001. Heat flow scaling for mantle convection below a conducting lid: resolving seemingly inconsistent modeling results regarding continental heat flow. *Geophysical Research Letters* 28, 1311–1314.
- Lizarralde, D., Axen, G.J., Brown, H.E., Fletcher, J.M., 2007. Variation in styles of rifting in the Gulf of California. *Nature* 448, 466–469. doi:10.1038/nature06035.
- Ludden, J., Hynes, A., 2000. The Abitibi-Grenville Lithoprobe transect part III: introduction. *Canadian Journal of Earth Sciences* 37, 115–116.
- MacGregor, I.D., 1974. The system MgO-Al₂O₃-SiO₂: Solubility of Al₂O₃ in enstatite for spinel and garnet peridotite compositions. *American Mineralogist* 59, 110–119.
- Matsukage, K.N., Nishihara, Y., Karato, S.-I., 2005. Seismological signature of chemical differentiation of Earth's upper mantle. *Journal of Geophysical Research* 110, B12305. doi:10.1029/2004JB003504.
- McKenzie, D.P., 1967. Some remarks on heat flow and gravity anomalies. *Journal of Geophysical Research* 72, 6261–6273.
- McKenzie, D.P., 1985. The extraction of magma from the crust and mantle. *Earth and Planetary Science Letters* 74, 81–91.
- McKenzie, D.P., 1989. Some remarks on the movement of small melt fractions in the mantle. *Earth and Planetary Science Letters* 95, 53–72.
- McKenzie, D., Jackson, J., Priestley, R., 2005. Thermal structure of oceanic and continental lithosphere. *Earth and Planetary Science Letters* 233, 337–349.
- Menzies, M.A., Weiming, F., Zhang, M., 1993. Paleozoic and Cenozoic lithoprobes and the loss of >120 km of Archean lithosphere, Sino-Korean craton, China. *Geological Society London, Special Publication* 76, 71–81.
- Michaut, C., Jaupart, C., 2007. Secular cooling and thermal structure of continental lithosphere. *Earth and Planetary Science Letters* 257, 83–96.
- Minster, J.B., Anderson, D.L., 1981. A model of dislocation-controlled rheology for the mantle. *Philosophical Transactions of the Royal Society of London* 299, 319–356.

- Montagner, J.-P., Kennett, B.L.N., 1996. How to reconcile body-wave and normal-mode reference Earth models? *Geophysical Journal International* 125, 229–248.
- Mooney W.D., 2005. Global crustal database. USGS compilation. <http://quake.wr.usgs.gov/research/structure/CrustalStructure/index.html>.
- Murase, T., Fukuyama, H., 1980. Shear wave velocity in partially molten peridotite at high pressures. Year Book Carnegie Institute, Washington, D.C., vol. 79, pp. 307–310.
- Murase, T., Kishiro, I., 1979. Compressional wave velocity in partially molten peridotite at high pressures. Year Book Carnegie Institute, Washington, D.C., vol. 78, pp. 559–562.
- Nimis, P., Taylor, W.R., 2000. Single clinopyroxene thermobarometry for garnet peridotites. Part 1. Calibration and testing of a Cr-in-Cpx barometer and an enstatite-in-Cpx thermometer. *Contributions to Mineralogy and Petrology* 139, 541–554.
- Niu, F.L., Levander, A., Cooper, C.M., Lee, C.-T., Lenardic, A., James, D., 2004. Seismic constraints on the depth keel beneath the and composition of the mantle Kaapvaal craton. *Earth and Planetary Science Letters* 224, 337–346.
- Nixon, P.H., Boyd, F.R., 1973. Petrogenesis of the granular and sheared ultrabasic nodule suite in kimberlites. In: Nixon, P.H. (Ed.), Lesotho kimberlites. Lesotho National Development Corporation, pp. 48–56.
- Nolet, G., Zielhuis, A., 1994. Low S velocities under the Tornquist–Teisseyre zone: evidence from water injection into the transition zone by subduction. *Journal of Geophysical Research* 99, 15813–15820.
- Nyblade, A.A., Pollack, H.N., 1993. A global analysis of heat flow from Precambrian terrains: implications for the thermal structure of Archean and Proterozoic lithosphere. *Journal of Geophysical Research* 98, 12207–12218.
- O'Neill, H.S.C., Wood, B.J., 1979. An empirical study of Fe–Mg partitioning between garnet and olivine and its calibration as a geothermometer. *Contributions to Mineralogy and Petrology* 70, 59–70.
- Pearson, D.G., Carlson, R.W., Shirey, S.B., Boyd, F.R., Nixon, P.H., 1995. Stabilization of Archean lithospheric mantle: a Re–Os isotope study of peridotite xenoliths from the Kaapvaal Craton. *Earth and Planetary Science Letters* 134, 341–357.
- Perry, H.K.C., Forte, A.M., Eaton, D.W.S., 2003. Upper mantle thermochemical structure beneath North America from seismic-geodynamic flow models. *Geophysical Journal International* 154, 279–299.
- Perry, H.K.C., Jaupart, C., Mareschal, J.-C., Bienfait, G., 2006. Crustal heat production in the Superior Province, Canadian Shield, and in North America inferred from heat flow data. *Journal of Geophysical Research* 111, B04401. doi:10.1029/2005JB003893.
- Petit, C., Koulakov, I., Deverchere, J., 1998. Velocity structure around the Baikal rift zone from teleseismic and local earthquake traveltimes and geodynamic implications. *Tectonophysics* 296, 125–144.
- Pinet, C., Jaupart, C., 1987. The vertical distribution of radiogenic heat production in the Precambrian crust of Norway and Sweden; geothermal implications. *Geophysical Research Letters* 14, 260–263.
- Plomerová, J., Kouba, D., Babuška, V., 2002. Mapping the lithosphere–asthenosphere boundary (LAB) through changes in seismic anisotropy. *Tectonophysics* 358, 175–186.
- Pollack, H.N., Chapman, D.S., 1977. On the regional variation of heat flow, geotherms, and lithospheric thickness. *Tectonophysics* 38, 279–296.
- Pollack, H.N., Hurter, S.J., Johnson, J.R., 1993. Heat flow from the Earth's interior: analysis of the global data set. *Reviews of Geophysics* 31, 267–280.
- Popp, T., Kern, H., 1993. Thermal dehydration reactions characterized by combined measurements of electrical conductivity and elastic wave velocities. *Earth and Planetary Science Letters* 120, 43–57.
- Priestley, K., Debayle, E., 2003. Seismic evidence for a moderately thick lithosphere beneath the Siberian platform. *Geophysical Research Letters* 30 (3), 1118. doi:10.1029/2002GL015931.
- Priestley, K., McKenzie, D., Debayle, E., 2006. The state of the upper mantle beneath southern Africa. *Tectonophysics* 416, 101–112.
- Revelle, R., Maxwell, A.E., 1952. Heat flow through the floor of the eastern North Pacific Ocean. *Nature* 170, 199–200.
- Ritsemá, J., van Heijst, H., 2000. New seismic model of the upper mantle beneath Africa. *Geology* 28, 63–66.
- Ritzwoller, M.H., Lavelly, E.M., 1995. Three-dimensional seismic models of the Earth's mantle. *Reviews of Geophysics* 33, 1–66.
- Röhm, A.H.E., Snieder, R., Goes, S., Trampert, J., 2000. Thermal structure of continental upper mantle inferred from S-wave velocity and surface heat flow. *Earth and Planetary Science Letters* 181, 395–407.
- Roy, R.F., Blackwell, D.D., Birch, F., 1968. Heat generation of plutonic rocks and continental heat flow provinces. *Earth and Planetary Science Letters* 5, 1–12.
- Rudnick, L.R., Nyblade, A.A., 1999. The thickness and heat production of Archean lithosphere: constraints from xenolith thermobarometry and surface heat flow. In: Fei, Y., Bertka, C.M., Mysen, B.O. (Eds.), *Mantle petrology: Field observations and high pressure experimentation: A tribute to Francis R. (Joe) Boyd*. Chemical Society Special Publication, vol. 6, pp. 3–12.
- Sato, H., Sacks, I.S., 1989. Anelasticity and thermal structure of the oceanic mantle: temperature calibration with heat flow data. *Journal of Geophysical Research* 94, 5705–5715.
- Sato, H., Sacks, I.S., Murase, T., 1989. The use of laboratory velocity data for estimating temperature and partial melt fraction in the low-velocity zone: comparison with heat flow and electrical studies. *Journal of Geophysical Research* 94, 5689–5704.
- Sclater, J.G., Jaupart, C., Galson, D., 1980. The heat flow through oceanic and continental crust and the heat loss of the Earth. *Reviews of Geophysics and Space Physics* 18, 269–311.
- Shapiro, N.M., Ritzwoller, M.H., 2002. Monte-Carlo inversion for a global shear velocity model of the crust and upper mantle. *Geophysical Journal International* 151, 1–18.
- Shirey, S.B., Harris, J.W., Richardson, S.H., Fouch, M.J., James, D.E., Cartigny, P., Deines, P., Viljoen, F., 2003. Regional patterns in the paragenesis and age of inclusions in diamond, diamond composition, and the lithospheric seismic structure of Southern Africa. *Lithos* 71, 243–258.
- Simons, F.J., Zielhuis, A., van der Hilst, R.D., 1999. The deep structure of the Australian continent from surface wave tomography. *Lithos* 48, 17–43.
- Sleep, N.H., 2003. Geodynamic implications of xenolith geotherms. *Geochemistry, Geophysics and Geosystems* 4 (9), 1079. doi:10.1029/2003GC000511.
- Sobolev, S.V., Zeyen, H., Stoll, G., Werling, F., Altherr, R., Fuchs, K., 1996. Upper mantle temperatures from teleseismic tomography of French Massif Central including effects of composition, mineral reactions, anharmonicity, anelasticity and partial melt. *Earth and Planetary Science Letters* 139, 147–163.
- Sumino, Y., Anderson, O.L., 1982. Elastic constants in minerals. In: Carmichael, R.S. (Ed.), *CRC Handbook of Physical Properties of Rocks*. CRC Press, Boca Raton, Fla., pp. 39–138.
- Tozer, D.C., 1981. The mechanical and electrical properties of earth's asthenosphere. *Physics of the Earth and Planetary Interior* 25, 280–296.
- Trampert, J., Woodhouse, J.H., 1995. Global phase velocity maps of Love and Rayleigh waves between 40 and 150 s. *Geophysical Journal International* 122, 675–690.
- Uffen, R.J., 1952. A method of estimating the melting-point gradient in the earth's mantle. *Transactions of American Geophysical Union* 33, 893–896.
- van der Lee, S., 2002. High-resolution estimates of lithospheric thickness from Missouri to Massachusetts, USA. *Earth and Planetary Science Letters* 203, 15–23.
- van Gerven, L., Deschamps, F., van der Hilst, R.D., 2004. Geophysical evidence for chemical variations in the Australian Continental Mantle. *Geophysical Research Letters* 31 Article Number: L17607.
- Wang, Y., Mareschal, J.-C., 1999. Elastic thickness of the lithosphere in the central Canadian Shield. *Geophysical Research Letters* 26, 3033–3036.
- Watts, A.B., 1978. An analysis of isostasy in the world's oceans. 1. Hawaiian–Emperor seamount chain. *Journal of Geophysical Research* 83, 5989–6004.
- Watts, A.B., 1999. *Isostasy and flexure of the lithosphere*. Cambridge University Press.
- Watts, A.B., 2001. *Isostasy and flexure of the lithosphere*. Cambridge University Press. 458 pp.
- Watts, A.B., Lamb, S.H., Fairhead, J.D., Dewey, J.F., 1995. Lithospheric flexure and bending of the central Andes. *Earth and Planetary Science Letters* 134 (1–2), 9–21.
- Woodland, A.B., Koch, M., 2003. Variation in oxygen fugacity with depth in the upper mantle beneath the Kaapvaal craton, Southern Africa. *Earth and Planetary Science Letters* 214, 295–310.
- Zhao, M., Langston, C.A., Nyblade, A.A., Owens, T.J., 1999. Upper mantle velocity structure beneath southern Africa from modeling regional seismic data. *Journal of Geophysical Research* 104, 4783–4794.
- Zhang, Y.-S., Tanimoto, T., 1993. High-resolution global upper mantle structure and plate tectonics. *Journal of Geophysical Research* 98, 9793–9823.